Structural Engineering and Mechanics, Vol. 39, No. 1 (2011) 47-75

DOI: http://dx.doi.org/10.12989/sem.2011.39.1.047

An accurate substructural synthesis approach to random responses

Z.G. Ying*[1], W.Q. Zhu[1], S.Q. Ye[2] and Y.Q. Ni[2]

[1]*Department of Mechanics, School of Aeronautics and Astronautics, Zhejiang University, Hangzhou 310027, P.R. China*
[2]*Department of Civil and Structural Engineering, The Hong Kong Polytechnic University, Kowloon, Hong Kong*

(Received June 29, 2010, Accepted February 22, 2011)

Abstract. An accurate substructural synthesis method including random responses synthesis, frequency-response functions synthesis and mid-order modes synthesis is developed based on rigorous substructure description, dynamic condensation and coupling. An entire structure can firstly be divided into several substructures according to different functions, geometric and dynamic characteristics. Substructural displacements are expressed exactly by retained mid-order fixed-interfacial normal modes and residual constraint modes. Substructural interfacial degree-of-freedoms are eliminated by interfacial displacements compatibility and forces equilibrium between adjacent substructures. Then substructural mode vibration equations are coupled to form an exact-condensed synthesized structure equation, from which structural mid-order modes are calculated accurately. Furthermore, substructural frequency-response function equations are coupled to yield an exact-condensed synthesized structure vibration equation in frequency domain, from which the generalized structural frequency-response functions are obtained. Substructural frequency-response functions are calculated separately by using the generalized frequency-response functions, which can be assembled into an entire-structural frequency-response function matrix. Substructural power spectral density functions are expressed by the exact-synthesized substructural frequency-response functions, and substructural random responses such as correlation functions and mean-square responses can be calculated separately. The accuracy and capacity of the proposed substructure synthesis method is verified by numerical examples.

Keywords: substructural synthesis; fixed interface substructure; random response; frequency-response function; mid-order mode

1. Introduction

For the dynamics analysis of large complicated structures in aerospace, mechanical and structural engineering, the dynamic substructuring techniques have been presented and applied effectively, which make substructures modeled and analyzed independently and are suitable to structural modification and optimization. The substructural mode synthesis method (Hurty 1965, Craig and Bampton 1968, Hou 1969, Meirovitch and Hale 1981, Greif 1986, Craig 1995, Qiu *et al.* 1997) combines the dynamic substructuring and mode analysis so as to possess their advantages, in

*Corresponding author, Professor, E-mail: yingzg@zju.edu.cn

particular, the high reduction of structural degree-of-freedom (DOF) and good asymptotic approximation to structural vibration. The two important steps of the substructural mode synthesis procedure are the substructural mode definition and description and the substructural models coupling, in which the DOF reduction and accuracy of a synthesized structure are concerned.

Many engineering structures such as in mechanical and structural engineering fields are subjected inevitably to random excitations, and structural responses are random processes with wide frequency band. The mid-order mode components of structural responses are necessary to be taken into account. In recent years, a dynamic substructuring technique for frequency-response functions in the medium-frequency range has been presented based on the mechanical energy operator (Soize and Mziou 2003) and the substructural proper orthogonal decomposition for parameter uncertainty (Sarkar and Ghanem 2003). A substructural dynamic modeling approach for short wave propagation has been given under certain synthesized-structural modal frequency accuracy (Barauskas and Barauskiene 2004). The mid-frequency vibration of a structure coupled with long-wave and short-wave substructures has been analyzed in terms of frequency response and power transmission (Ji *et al.* 2006). The other development in dynamic substructuring includes the frequency response analysis of viscoelastic structures (Qian and Hansen 1995), the high-frequency response in specified frequency interval (Ko and Bai 2008) and the dynamic response algorithm with time discretization (Tsuei and Yee 1990), as well as the structural decomposition and substructural connection (for example, Petrini *et al.* 2010, Liu 2010). An approach to simulate large-scale structural systems that combines a simplified global model with multiple detailed component models has also been presented (Chen and Iranata 2008). In general, the effects of substructural modes truncation or incompleteness on substructural description, entire structural normal modes and frequency response were neglected in the mid-frequency vibration analysis while interface DOFs were retained in the synthesized structure. Since structural mid-order modes are more sensitive to description and synthesis errors than structural lower-order modes, the exact substructure description condensed through dynamic relations and the exact synthesis with interface DOFs eliminated through displacements compatibility and forces equilibrium will improve the substructural synthesis and random response.

The purpose of this paper is to develop an accurate substructural synthesis method including mid-order modes synthesis, frequency-response functions synthesis and random responses synthesis based on rigorous substructural description, dynamic condensation and coupling. Firstly, substructural displacements are expressed exactly by fixed-interfacial normal modes and static constraint modes. Then substructural DOFs are reduced by eliminating lower/higher-order normal modes according to rigorous mode vibration equations, so that the substructural lower/higher-order normal modes and static constraint modes are replaced by the exact residual constraint modes. Secondly, substructural mode vibration equations are coupled by the exact interfacial displacements compatibility and forces equilibrium to form an exact-condensed synthesized structure equation without interface DOFs. Structural mid-order normal modes are obtained by the synthesized-structure mode analysis. Thirdly, substructural frequency-response function equations are coupled by the exact interfacial displacements compatibility and forces equilibrium to yield an exact-condensed structure vibration equation in frequency domain. The generalized synthesized frequency-response functions are obtained by solving this equation, and then the substructural frequency-response functions are obtained, which can be used for structural dynamic characteristics and response analysis. Fourthly, substructural power spectral density functions are expressed by the exact-synthesized substructural frequency-response functions and substructure dynamics, and then substructural correlation functions including mean-square values of displacements and accelerations are calculated by using the exact-synthesized substructural power spectral density functions respectively, which can form structural response statistics. Finally, numerical examples are given to illustrate the accuracy and capacity of the proposed substructural synthesis method in terms of structural mid-order modes, frequency-response functions and mean-square responses.

2. Substructure description and exact condensation

According to dynamic substructuring, a large structure is firstly divided into several smaller substructures based on different functions, geometric and dynamic characteristics (Craig 1995). The differential equation of motion of an undamped substructure can be expressed as

$$\mathbf{m}\ddot{\mathbf{X}} + \mathbf{k}\mathbf{X} = \mathbf{f} \tag{1}$$

where $\mathbf{X}$ is the substructural displacement vector, $\mathbf{m}$, $\mathbf{k}$ and $\mathbf{f}$ are the substructural positive-definite symmetric mass matrix, positive-semidefinite symmetric stiffness matrix and external force vector, respectively. In terms of substructural interface DOFs and non-interface DOFs, Eq. (1) is partitioned into

$$\begin{bmatrix} \mathbf{m}_{II} & \mathbf{m}_{IJ} \\ \mathbf{m}_{JI} & \mathbf{m}_{JJ} \end{bmatrix} \begin{Bmatrix} \ddot{\mathbf{X}}_I \\ \ddot{\mathbf{X}}_J \end{Bmatrix} + \begin{bmatrix} \mathbf{k}_{II} & \mathbf{k}_{IJ} \\ \mathbf{k}_{JI} & \mathbf{k}_{JJ} \end{bmatrix} \begin{Bmatrix} \mathbf{X}_I \\ \mathbf{X}_J \end{Bmatrix} = \begin{Bmatrix} \mathbf{f}_I \\ \mathbf{f}_J \end{Bmatrix} \tag{2}$$

where subscripts I and J denote substructural non-interface DOFs and interface DOFs, respectively. For the structural and substructural free vibrations, the non-interface force vector $\mathbf{f}_I = 0$. In this case, the non-interfacial fixed constraint DOFs have been eliminated and the non-interface stiffness matrix $\mathbf{k}_{II}$ is assumed as positive definite.

After substructures are separated from an entire structure, the interfaces between original adjacent substructures can be treated as free or fixed to form correspondingly free interface substructures or fixed interface substructures for dynamics analysis (Greif 1986, Hurty 1965, Craig and Bampton 1968, Hou 1969). Consider the substructure with interface DOFs fixed or fixed-interface substructure. Then the interface displacement vector is $\mathbf{X}_J = 0$. The free vibration equation of the fixed-interface substructure is derived from Eq. (2) as

$$\mathbf{m}_{II}\ddot{\mathbf{X}}_I + \mathbf{k}_{II}\mathbf{X}_I = 0 \tag{3}$$

The eigenvalue equation corresponding to Eq. (3) is

$$(\mathbf{k}_{II} - \omega^2 \mathbf{m}_{II})\boldsymbol{\phi}_I = 0 \tag{4}$$

where ω and $\boldsymbol{\phi}_I$ are the vibration frequency and shape vector, respectively. The natural frequency ω_i and normal mode $\boldsymbol{\phi}_{Ii}$ ($i = 1, 2, \ldots$) of the fixed-interface substructure can be obtained by solving Eq. (4). According to the order of the natural frequencies, the normal mode vectors are assembled into lower-order normal mode matrix $\boldsymbol{\varphi}_{Il}$, mid-order normal mode matrix $\boldsymbol{\varphi}_{Im}$ and higher-order normal mode matrix $\boldsymbol{\varphi}_{Ih}$, which satisfy the orthogonality relations such as normalized with respect to the mass matrix. The fixed-interfacial substructural normal modes can be used for describing substructure motion. For the original substructure with unfixed interface, the fixed-interfacial substructural normal mode matrices are augmented by supplementing zeros to interface DOFs as

$$\boldsymbol{\varphi} = [\boldsymbol{\varphi}_l \ \ \boldsymbol{\varphi}_m \ \ \boldsymbol{\varphi}_h] \tag{5a}$$

$$\boldsymbol{\varphi}_l = \begin{bmatrix} \boldsymbol{\varphi}_{Il} \\ 0 \end{bmatrix}, \quad \boldsymbol{\varphi}_m = \begin{bmatrix} \boldsymbol{\varphi}_{Im} \\ 0 \end{bmatrix}, \quad \boldsymbol{\varphi}_h = \begin{bmatrix} \boldsymbol{\varphi}_{Ih} \\ 0 \end{bmatrix} \tag{5b,c,d}$$

The substructure modes satisfy the orthogonality relations

$$\boldsymbol{\varphi}^T\mathbf{m}\boldsymbol{\varphi} = \mathbf{I}, \ \boldsymbol{\varphi}^T\mathbf{k}\boldsymbol{\varphi} = \boldsymbol{\Lambda} \tag{6a,b}$$

$$\boldsymbol{\Lambda} = \mathrm{diag}[\boldsymbol{\Lambda}_l \ \ \boldsymbol{\Lambda}_m \ \ \boldsymbol{\Lambda}_h] = \mathrm{daig}[\omega_1^2 \ \ \omega_2^2 \ \ \ldots] \tag{6c}$$

where $\mathbf{I}$ is an identity matrix. However, the substructural normal modes $\boldsymbol{\varphi}$ are an incomplete set. The static constraint modes are generally chosen as the supplementary set, which are substructural static displacement vectors under only a unit displacement applied to each interface DOF. The static constraint mode matrix is

$$\boldsymbol{\varphi}_{co} = \begin{bmatrix} -\mathbf{k}_{II}^{-1}\mathbf{k}_{IJ} \\ \mathbf{I}_J \end{bmatrix} \tag{7}$$

where $\mathbf{I}_J$ is an identity matrix corresponding to interface DOFs. Obviously, the substructural normal modes $\boldsymbol{\varphi}$ and the static constraint modes $\boldsymbol{\varphi}_{co}$ are linearly independent and constitute a complete set. Then the substructure displacement vector can be expressed exactly by

$$\mathbf{X} = \boldsymbol{\varphi}_{co}\mathbf{u}_c + \boldsymbol{\varphi}_l\mathbf{u}_l + \boldsymbol{\varphi}_m\mathbf{u}_m + \boldsymbol{\varphi}_h\mathbf{u}_h \tag{8}$$

where $\mathbf{u}_c$, $\mathbf{u}_l$, $\mathbf{u}_m$ and $\mathbf{u}_h$ are substructural mode displacement vectors corresponding to modes $\boldsymbol{\varphi}_{co}$, $\boldsymbol{\varphi}_l$, $\boldsymbol{\varphi}_m$ and $\boldsymbol{\varphi}_h$, respectively.

Substituting displacement expression (8) into Eq. (1), premultiplying the resultant equation by the transposed mode matrix, using the orthogonality relations and free vibration condition $\mathbf{f}_I = 0$ yield

$$\boldsymbol{\varphi}_{co}^T\mathbf{m}(\boldsymbol{\varphi}_{co}\ddot{\mathbf{u}}_c + \boldsymbol{\varphi}_l\ddot{\mathbf{u}}_l + \boldsymbol{\varphi}_m\ddot{\mathbf{u}}_m + \boldsymbol{\varphi}_h\ddot{\mathbf{u}}_h) + \boldsymbol{\varphi}_{co}^T\mathbf{k}\boldsymbol{\varphi}_{co}\mathbf{u}_c = \mathbf{f}_J \tag{9a}$$

$$\boldsymbol{\varphi}_l^T\mathbf{m}\boldsymbol{\varphi}_{co}\ddot{\mathbf{u}}_c + \ddot{\mathbf{u}}_l + \boldsymbol{\Lambda}_l\mathbf{u}_l = 0 \tag{9b}$$

$$\boldsymbol{\varphi}_m^T\mathbf{m}\boldsymbol{\varphi}_{co}\ddot{\mathbf{u}}_c + \ddot{\mathbf{u}}_m + \boldsymbol{\Lambda}_m\mathbf{u}_m = 0 \tag{9c}$$

$$\boldsymbol{\varphi}_h^T\mathbf{m}\boldsymbol{\varphi}_{co}\ddot{\mathbf{u}}_c + \ddot{\mathbf{u}}_h + \boldsymbol{\Lambda}_h\mathbf{u}_h = 0 \tag{9d}$$

For the structural mode vibration or substructural harmonic vibration with frequency ω, Eq. (9) becomes through the Fourier transformation

$$\boldsymbol{\varphi}_{co}^T(\mathbf{k} - \omega^2\mathbf{m})\boldsymbol{\varphi}_{co}\mathbf{u}_c - \omega^2\boldsymbol{\varphi}_{co}^T\mathbf{m}(\boldsymbol{\varphi}_l\mathbf{u}_l + \boldsymbol{\varphi}_m\mathbf{u}_m + \boldsymbol{\varphi}_h\mathbf{u}_h) = \mathbf{f}_J \tag{10a}$$

$$(\Lambda_l - \omega^2 \mathbf{I}_l)\mathbf{u}_l - \omega^2 \varphi_l^T \mathbf{m} \varphi_{co} \mathbf{u}_c = 0 \tag{10b}$$

$$(\Lambda_m - \omega^2 \mathbf{I}_m)\mathbf{u}_m - \omega^2 \varphi_m^T \mathbf{m} \varphi_{co} \mathbf{u}_c = 0 \tag{10c}$$

$$(\Lambda_h - \omega^2 \mathbf{I}_h)\mathbf{u}_h - \omega^2 \varphi_h^T \mathbf{m} \varphi_{co} \mathbf{u}_c = 0 \tag{10d}$$

where $\mathbf{I}_l$, $\mathbf{I}_m$ and $\mathbf{I}_h$ are identity matrices corresponding to lower-order, mid-order and higher-order normal modes, respectively. In general, structural natural frequencies are separated into individual ones by substructural natural frequencies and the interval of the former contains that of the latter. For the structural mid-order mode vibration, substructural mid-order normal modes φ_m are correspondingly chosen as a basic mode set describing vibration according to the frequency interval concerned and the dominant excitation frequency band. Then the substructure DOFs in mode space can be reduced by eliminating substructural lower-order and higher-order normal modes (φ_l and φ_h), and the substructural lower-order and higher-order mode displacements ($\mathbf{u}_l$ and $\mathbf{u}_h$) can be expressed by the substructural static constraint modes with mode displacements ($\mathbf{u}_c$) according to Eqs. (10b) and (10d). By substituting the substructural lower-order and higher-order mode displacement expressions into Eq. (8), the substructural displacement vector is rigorously rewritten in the condensation form

$$\mathbf{X} = \varphi_c \mathbf{u}_c + \varphi_m \mathbf{u}_m \tag{11}$$

where the constraint mode matrix

$$\varphi_c(\omega^2) = \varphi_{co} + \omega^2(\psi_l + \psi_h)\mathbf{m}\varphi_{co} \tag{12}$$

$$\psi_l(\omega^2) = \varphi_l(\Lambda_l - \omega^2 \mathbf{I}_l)^{-1}\varphi_l^T, \quad \psi_h(\omega^2) = \varphi_h(\Lambda_h - \omega^2 \mathbf{I}_h)^{-1}\varphi_h^T \tag{13a,b}$$

The modes φ_c include the static constraint modes and the other part transformed from the lower-order and higher-order normal modes by the equivalence of displacements (8) and (11), which are called the exact residual constraint modes. Eq. (11) implies that the substructural mid-order normal modes φ_m and the exact residual constraint modes φ_c can exactly describe substructural harmonic vibration in a condensation form. According to the frequency interval concerned, the substructural higher-order or lower-order normal modes can also be combined into the mid-order normal modes by eliminating mode matrix φ_h or φ_l. The matrix $\psi_l + \psi_h$ represents the exact residual flexibility and can be rewritten as

$$\psi_l + \psi_h = \mathbf{G}(\omega^2) - \varphi_m(\Lambda_m - \omega^2 \mathbf{I}_m)^{-1}\varphi_m^T \tag{14a}$$

$$\mathbf{G}(\omega^2) = \begin{bmatrix} (\mathbf{k}_{II} - \omega^2 \mathbf{m}_{II})^{-1} & 0 \\ 0 & 0 \end{bmatrix} \tag{14b}$$

By taking the sub-vector of displacement vector (11) corresponding to interface DOFs, the substructural interface displacement obtained is

$$\mathbf{X}_J = \mathbf{u}_c \tag{15}$$

The substructural interface force is derived by substituting Eqs. (10b) and (10d) into Eq. (10a) and using the expression of the exact residual constraint modes (12) with (13), that is

$$\begin{aligned}\mathbf{f}_J &= \boldsymbol{\varphi}_{co}^T(\mathbf{k}-\omega^2\mathbf{m})\boldsymbol{\varphi}_c\mathbf{u}_c - \omega^2\boldsymbol{\varphi}_{co}^T\mathbf{m}\boldsymbol{\varphi}_m\mathbf{u}_m \\ &= \boldsymbol{\varphi}_c^T(\mathbf{k}-\omega^2\mathbf{m})\boldsymbol{\varphi}_c\mathbf{u}_c - \omega^2\boldsymbol{\varphi}_{co}^T\mathbf{m}\boldsymbol{\varphi}_m\mathbf{u}_m\end{aligned} \tag{16}$$

3. Substructures coupling for exact mid-order modes

The substructural synthesis is studied from the mid-order mode synthesis, frequency-response function synthesis to random response synthesis. Substructural mode vibration equations can be coupled by exact interfacial displacements compatibility and forces equilibrium to form an exact condensed structure equation, and then structural mid-order modes can be calculated accurately by the synthesized-structure mode analysis. For simplicity, here consider two adjacent substructures coupling, in which substructures α and β have a common interface. The coupling procedure can be extended to the case with more than two substructures.

According to Eq. (11), the two substructural displacement vectors are expressed in the exact condensation form

$$\mathbf{X}^\alpha = \boldsymbol{\varphi}_c^\alpha\mathbf{u}_c^\alpha + \boldsymbol{\varphi}_m^\alpha\mathbf{u}_m^\alpha = \boldsymbol{\varphi}^\alpha\mathbf{u}^\alpha \tag{17a}$$

$$\mathbf{X}^\beta = \boldsymbol{\varphi}_c^\beta\mathbf{u}_c^\beta + \boldsymbol{\varphi}_m^\beta\mathbf{u}_m^\beta = \boldsymbol{\varphi}^\beta\mathbf{u}^\beta \tag{17b}$$

where superscripts α and β denote substructures α and β, respectively, the substructural mode matrices and mode displacement vectors are

$$\boldsymbol{\varphi}^\alpha = [\boldsymbol{\varphi}_c^\alpha \;\; \boldsymbol{\varphi}_m^\alpha], \quad \boldsymbol{\varphi}^\beta = [\boldsymbol{\varphi}_c^\beta \;\; \boldsymbol{\varphi}_m^\beta] \tag{18a,b}$$

$$\mathbf{u}^\alpha = [\mathbf{u}_c^{\alpha T} \;\; \mathbf{u}_m^{\alpha T}]^T, \quad \mathbf{u}^\beta = [\mathbf{u}_c^{\beta T} \;\; \mathbf{u}_m^{\beta T}]^T \tag{19a,b}$$

For substructures α and β, the interface displacement (15) and interface force (16) are rewritten as

$$\mathbf{X}_J^\alpha = \mathbf{u}_c^\alpha, \quad \mathbf{X}_J^\beta = \mathbf{u}_c^\beta \tag{20a,b}$$

$$\mathbf{f}_J^\alpha = \boldsymbol{\varphi}_c^{\alpha T}(\mathbf{k}^\alpha-\omega^2\mathbf{m}^\alpha)\boldsymbol{\varphi}_c^\alpha\mathbf{u}_c^\alpha - \omega^2\boldsymbol{\varphi}_{co}^{\alpha T}\mathbf{m}^\alpha\boldsymbol{\varphi}_m^\alpha\mathbf{u}_m^\alpha \tag{21a}$$

$$\mathbf{f}_J^\beta = \boldsymbol{\varphi}_c^{\beta T}(\mathbf{k}^\beta-\omega^2\mathbf{m}^\beta)\boldsymbol{\varphi}_c^\beta\mathbf{u}_c^\beta - \omega^2\boldsymbol{\varphi}_{co}^{\beta T}\mathbf{m}^\beta\boldsymbol{\varphi}_m^\beta\mathbf{u}_m^\beta \tag{21b}$$

In the expressions (17)-(21), the generalized substructural mode displacements $\mathbf{u}^\alpha$ and $\mathbf{u}^\beta$ include DOFs relative to mid-order modes and interfaces, which can be condensed further.

According to the original entire structure, the adjacent substructure displacements need to satisfy the compatibility condition at the interface, which gives

$$\mathbf{X}_J^{\alpha} = \mathbf{X}_J^{\beta} \tag{22}$$

Substituting the substructural interface displacements (20a) and (20b) into condition (22) yields

$$\mathbf{u}_c^{\alpha} = \mathbf{u}_c^{\beta} \tag{23}$$

Similarly, the adjacent substructure forces need to satisfy the equilibrium relation at the interface, that is

$$\mathbf{f}_J^{\alpha} + \mathbf{f}_J^{\beta} = 0 \tag{24}$$

Substituting the substructural interface forces (21a) and (21b) into relation (24) and using Eq. (23) yield

$$\mathbf{u}_c^{\alpha} = \mathbf{u}_c^{\beta} = \mathbf{g}_c(\mathbf{m}_{cm}^{\alpha}\mathbf{u}_m^{\alpha} + \mathbf{m}_{cm}^{\beta}\mathbf{u}_m^{\beta}) \tag{25}$$

where

$$\mathbf{m}_{cm}^{\alpha} = \boldsymbol{\varphi}_{co}^{\alpha T}\mathbf{m}^{\alpha}\boldsymbol{\varphi}_m^{\alpha}, \quad \mathbf{m}_{cm}^{\beta} = \boldsymbol{\varphi}_{co}^{\beta T}\mathbf{m}^{\beta}\boldsymbol{\varphi}_m^{\beta} \tag{26a,b}$$

$$\mathbf{g}_c(\omega^2) = \omega^2[\boldsymbol{\varphi}_c^{\alpha T}(\mathbf{k}^{\alpha} - \omega^2\mathbf{m}^{\alpha})\boldsymbol{\varphi}_c^{\alpha} + \boldsymbol{\varphi}_c^{\beta T}(\mathbf{k}^{\beta} - \omega^2\mathbf{m}^{\beta})\boldsymbol{\varphi}_c^{\beta}]^{-1} \tag{27}$$

Eq. (25) implies that the substructural mode displacements $\mathbf{u}_c^{\alpha}$ and $\mathbf{u}_c^{\beta}$ can be expressed by adjacent-substructural mid-order mode displacements $\mathbf{u}_m^{\alpha}$ and $\mathbf{u}_m^{\beta}$, and then the substructural interface DOFs can be eliminated further based on the substructural displacements compatibility and forces equilibrium. According to Eq. (25), the exact condensation transformations for substructural mode displacements are obtained as

$$\mathbf{u}^{\alpha} = \mathbf{T}^{\alpha}\mathbf{U}, \quad \mathbf{u}^{\beta} = \mathbf{T}^{\beta}\mathbf{U} \tag{28a,b}$$

where adjacent-substructural mid-order mode displacement vector $\mathbf{U}$, and substructural displacement condensation transformation matrices $\mathbf{T}^{\alpha}$ and $\mathbf{T}^{\beta}$ are

$$\mathbf{U} = [\mathbf{u}_m^{\alpha T} \;\; \mathbf{u}_m^{\beta T}]^T \tag{29}$$

$$\mathbf{T}^{\alpha}(\omega^2) = \begin{bmatrix} \mathbf{g}_c\mathbf{m}_{cm}^{\alpha} & \mathbf{g}_c\mathbf{m}_{cm}^{\beta} \\ \mathbf{I}_m^{\alpha} & 0 \end{bmatrix}, \quad \mathbf{T}^{\beta}(\omega^2) = \begin{bmatrix} \mathbf{g}_c\mathbf{m}_{cm}^{\alpha} & \mathbf{g}_c\mathbf{m}_{cm}^{\beta} \\ 0 & \mathbf{I}_m^{\beta} \end{bmatrix} \tag{30a,b}$$

Substituting the exact substructural displacements (17a) and (17b) into Eq. (1) for substructures α and β, premultiplying the resultant equations by the transposed mode matrices $\boldsymbol{\varphi}^{\alpha T}$ and $\boldsymbol{\varphi}^{\beta T}$, and then converting them into ones for the substructural harmonic vibration with frequency ω, respectively, yield

$$(\mathbf{K}^{\alpha} - \omega^2\mathbf{M}^{\alpha})\mathbf{u}^{\alpha} = \mathbf{F}^{\alpha} \tag{31a}$$

$$(\mathbf{K}^{\beta} - \omega^2\mathbf{M}^{\beta})\mathbf{u}^{\beta} = \mathbf{F}^{\beta} \tag{31b}$$

where

$$\mathbf{K}^{\alpha}(\omega^2) = \begin{bmatrix} \boldsymbol{\varphi}_{co}^{\alpha T}\mathbf{k}^{\alpha}\boldsymbol{\varphi}_{co}^{\alpha} & 0 \\ 0 & \boldsymbol{\Lambda}_m^{\alpha} \end{bmatrix}, \quad \mathbf{K}^{\beta}(\omega^2) = \begin{bmatrix} \boldsymbol{\varphi}_{co}^{\beta T}\mathbf{k}^{\beta}\boldsymbol{\varphi}_{co}^{\beta} & 0 \\ 0 & \boldsymbol{\Lambda}_m^{\beta} \end{bmatrix} \tag{32a,b}$$

$$\mathbf{M}^{\alpha}(\omega^2) = \begin{bmatrix} \boldsymbol{\varphi}_{c}^{\alpha T}\mathbf{m}^{\alpha}\boldsymbol{\varphi}_{c}^{\alpha} & \mathbf{m}_{cm}^{\alpha} \\ \mathbf{m}_{cm}^{\alpha \mathrm{T}} & \mathbf{I}_m^{\alpha} \end{bmatrix}, \quad \mathbf{M}^{\beta}(\omega^2) = \begin{bmatrix} \boldsymbol{\varphi}_{c}^{\beta T}\mathbf{m}^{\beta}\boldsymbol{\varphi}_{c}^{\beta} & \mathbf{m}_{cm}^{\beta} \\ \mathbf{m}_{cm}^{\beta T} & \mathbf{I}_m^{\beta} \end{bmatrix} \tag{33a,b}$$

$$\mathbf{F}^{\alpha} = \begin{Bmatrix} \mathbf{f}_J^{\alpha} \\ 0 \end{Bmatrix}, \quad \mathbf{F}^{\beta} = \begin{Bmatrix} \mathbf{f}_J^{\beta} \\ 0 \end{Bmatrix} \tag{34a,b}$$

Further substituting the exact condensation transformations (28a) and (28b) into Eqs. (31a) and (31b), and premultiplying the resultant equations by the transposed transformation matrices $\mathbf{T}^{\alpha T}$ and $\mathbf{T}^{\beta T}$, respectively, give

$$\mathbf{T}^{\alpha T}(\mathbf{K}^{\alpha} - \omega^2\mathbf{M}^{\alpha})\mathbf{T}^{\alpha}\mathbf{U} = \mathbf{T}^{\alpha T}\mathbf{F}^{\alpha} \tag{35a}$$

$$\mathbf{T}^{\beta T}(\mathbf{K}^{\beta} - \omega^2\mathbf{M}^{\beta})\mathbf{T}^{\beta}\mathbf{U} = \mathbf{T}^{\beta T}\mathbf{F}^{\beta} \tag{35b}$$

Eqs. (35a) and (35b) exactly describe substructural harmonic vibration with frequency ω corresponding to entire structural mode vibration, in which DOFs relative to substructural lower/higher-order normal modes and interfaces have been eliminated or only DOFs relative to substructural mid-order normal modes have been retained. The substructural lower/higher-order normal modes and constraint modes relative to interface DOFs have been involved in the coefficients of Eq. (35) by $\boldsymbol{\varphi}_l$, $\boldsymbol{\varphi}_h$ and $\boldsymbol{\varphi}_{co}$.

By assembling substructural Eqs. (35a) and (35b), the entire-structural mode vibration equation is obtained in the exact condensation form

$$(\mathbf{K} - \omega^2\mathbf{M})\mathbf{U} = \mathbf{F} \tag{36}$$

where the synthesized structure stiffness matrix **K**, mass matrix **M** and force vector **F** are

$$\mathbf{K} = \mathbf{T}^{\alpha T}\mathbf{K}^{\alpha}\mathbf{T}^{\alpha} + \mathbf{T}^{\beta T}\mathbf{K}^{\beta}\mathbf{T}^{\beta} \tag{37a}$$

$$\mathbf{M} = \mathbf{T}^{\alpha T}\mathbf{M}^{\alpha}\mathbf{T}^{\alpha} + \mathbf{T}^{\beta T}\mathbf{M}^{\beta}\mathbf{T}^{\beta} \tag{37b}$$

$$\mathbf{F} = \mathbf{T}^{\alpha T}\mathbf{F}^{\alpha} + \mathbf{T}^{\beta T}\mathbf{F}^{\beta} \tag{37c}$$

It can be verified that $\mathbf{F} = 0$ by substituting Eqs. (30) and (34) into Eq. (37c) and using relation (24). Then the synthesized structure Eq. (36) becomes

$$(\mathbf{K} - \omega^2\mathbf{M})\mathbf{U} = 0 \tag{38}$$

Structural mid-order natural frequencies can be obtained by solving eigenequation (38) which is nonlinear one with respect to frequency ω^2. Thus the exact DOF reduction of the structural eigenproblem induces the nonlinearity of the reduced eigenproblem with respect to frequency. Eq. (38) can be solved by iteration procedures, for instance, the shifting frequency and subspace iteration algorithm. The convergence and accuracy of an iterating solution depend on not only the algorithm but also the initial approximate values. Note that the synthesized structure stiffness **K** and mass **M** are functions of frequency ω. Letting $\omega = 0$ yields

$$\mathbf{K} = \begin{bmatrix} \mathbf{\Lambda}_m^\alpha & 0 \\ 0 & \mathbf{\Lambda}_m^\beta \end{bmatrix}, \quad \mathbf{M} = \begin{bmatrix} \mathbf{I}_m^\alpha & 0 \\ 0 & \mathbf{I}_m^\beta \end{bmatrix} \tag{39a,b}$$

which can be used as coefficients of Eq. (38) to obtain the first approximate results. Then replacing $\boldsymbol{\varphi}_c$ with $\boldsymbol{\varphi}_{co}$ and simplifying Eq. (38) yield

$$\mathbf{K} = \begin{bmatrix} \mathbf{\Lambda}_m^\alpha & 0 \\ 0 & \mathbf{\Lambda}_m^\beta \end{bmatrix} \tag{40a}$$

$$\mathbf{M} = \begin{bmatrix} \mathbf{I}_m^\alpha + \omega^2 \mathbf{m}_{cm}^{\alpha T} \mathbf{k}_{cc} \mathbf{m}_{cm}^\alpha & \mathbf{m}_{cm}^{\alpha T} \mathbf{k}_{cc} \mathbf{m}_{cm}^\beta \\ \mathbf{m}_{cm}^{\beta T} \mathbf{k}_{cc} \mathbf{m}_{cm}^\alpha & \mathbf{I}_m^\beta + \omega^2 \mathbf{m}_{cm}^{\beta T} \mathbf{k}_{cc} \mathbf{m}_{cm}^\beta \end{bmatrix} \tag{40b}$$

$$\mathbf{k}_{cc} = (\boldsymbol{\varphi}_{co}^{\alpha T} \mathbf{k}^\alpha \boldsymbol{\varphi}_{co}^\alpha + \boldsymbol{\varphi}_{co}^{\beta T} \mathbf{k}^\beta \boldsymbol{\varphi}_{co}^\beta)^{-1} \tag{40c}$$

which can be used as modified coefficients to obtain the second approximate results. These results will be better initial values for the original eigenequation (38).

4. Substructures coupling for exact frequency-response functions

The frequency-response functions can be used for describing structural dynamic characteristics and calculating structural dynamic response. Here the structural frequency-response functions are obtained by two main steps, that is, deriving the generalized frequency-response functions of the exact condensed structure and expressing the frequency-response functions of the original structure or each substructure.

For simplicity, consider two adjacent substructures coupling, in which substructures α and β have a common interface. The coupling procedure can be extended to the case with more than two substructures. The differential equations of motion of the two substructures with damping are given by

$$\mathbf{m}^\alpha \ddot{\mathbf{X}}^\alpha + \mathbf{c}^\alpha \dot{\mathbf{X}}^\alpha + \mathbf{k}^\alpha \mathbf{X}^\alpha = \mathbf{f}^\alpha \tag{41a}$$

$$\mathbf{m}^\beta \ddot{\mathbf{X}}^\beta + \mathbf{c}^\beta \dot{\mathbf{X}}^\beta + \mathbf{k}^\beta \mathbf{X}^\beta = \mathbf{f}^\beta \tag{41b}$$

where $\mathbf{c}^\alpha$ and $\mathbf{c}^\beta$ are symmetric damping matrices of substructures α and β, respectively, the other symbols are as indicated in the preceding. According to expression (8), the substructural displacement vectors can be given exactly by

$$\mathbf{X}^{\alpha} = \boldsymbol{\varphi}_{co}^{\alpha}\mathbf{u}_{c}^{\alpha} + \boldsymbol{\varphi}_{l}^{\alpha}\mathbf{u}_{l}^{\alpha} + \boldsymbol{\varphi}_{m}^{\alpha}\mathbf{u}_{m}^{\alpha} + \boldsymbol{\varphi}_{h}^{\alpha}\mathbf{u}_{h}^{\alpha} \tag{42a}$$

$$\mathbf{X}^{\beta} = \boldsymbol{\varphi}_{co}^{\beta}\mathbf{u}_{c}^{\beta} + \boldsymbol{\varphi}_{l}^{\beta}\mathbf{u}_{l}^{\beta} + \boldsymbol{\varphi}_{m}^{\beta}\mathbf{u}_{m}^{\beta} + \boldsymbol{\varphi}_{h}^{\beta}\mathbf{u}_{h}^{\beta} \tag{42b}$$

Eqs. (41) and (42) are converted by the Fourier transformation into

$$(\mathbf{k}^{\alpha} + j\omega\mathbf{c}^{\alpha} - \omega^{2}\mathbf{m}^{\alpha})\overline{\mathbf{X}}^{\alpha} = \overline{\mathbf{f}}^{\alpha} \tag{43a}$$

$$(\mathbf{k}^{\beta} + j\omega\mathbf{c}^{\beta} - \omega^{2}\mathbf{m}^{\beta})\overline{\mathbf{X}}^{\beta} = \overline{\mathbf{f}}^{\beta} \tag{43b}$$

$$\overline{\mathbf{X}}^{\alpha} = \boldsymbol{\varphi}_{co}^{\alpha}\overline{\mathbf{u}}_{c}^{\alpha} + \boldsymbol{\varphi}_{l}^{\alpha}\overline{\mathbf{u}}_{l}^{\alpha} + \boldsymbol{\varphi}_{m}^{\alpha}\overline{\mathbf{u}}_{m}^{\alpha} + \boldsymbol{\varphi}_{h}^{\alpha}\overline{\mathbf{u}}_{h}^{\alpha} \tag{44a}$$

$$\overline{\mathbf{X}}^{\beta} = \boldsymbol{\varphi}_{co}^{\beta}\overline{\mathbf{u}}_{c}^{\beta} + \boldsymbol{\varphi}_{l}^{\beta}\overline{\mathbf{u}}_{l}^{\beta} + \boldsymbol{\varphi}_{m}^{\beta}\overline{\mathbf{u}}_{m}^{\beta} + \boldsymbol{\varphi}_{h}^{\beta}\overline{\mathbf{u}}_{h}^{\beta} \tag{44b}$$

where the over-bar represents the Fourier transformation and $j = \sqrt{-1}$. Substituting the transformed substructure displacements (44a) and (44b) into Eqs. (43a) and (43b), respectively, premultiplying the resultant equations by the transposed lower-order and higher-order mode matrices, and using the orthogonality relations (6) yield

$$\overline{\mathbf{u}}_{l}^{\alpha} = (\boldsymbol{\Lambda}_{l}^{\alpha} + j\omega\boldsymbol{\varphi}_{l}^{\alpha T}\mathbf{c}^{\alpha}\boldsymbol{\varphi}_{l}^{\alpha} - \omega^{2}\mathbf{I}_{l}^{\alpha})^{-1}[(-j\omega\boldsymbol{\varphi}_{l}^{\alpha T}\mathbf{c}^{\alpha}\boldsymbol{\varphi}_{co}^{\alpha} + \omega^{2}\boldsymbol{\varphi}_{l}^{\alpha T}\mathbf{m}^{\alpha}\boldsymbol{\varphi}_{co}^{\alpha})\overline{\mathbf{u}}_{c}^{\alpha} + \boldsymbol{\varphi}_{l}^{\alpha T}\overline{\mathbf{f}}^{\alpha}] \tag{45a}$$

$$\overline{\mathbf{u}}_{h}^{\alpha} = (\boldsymbol{\Lambda}_{h}^{\alpha} + j\omega\boldsymbol{\varphi}_{h}^{\alpha T}\mathbf{c}^{\alpha}\boldsymbol{\varphi}_{h}^{\alpha} - \omega^{2}\mathbf{I}_{h}^{\alpha})^{-1}[(-j\omega\boldsymbol{\varphi}_{h}^{\alpha T}\mathbf{c}^{\alpha}\boldsymbol{\varphi}_{co}^{\alpha} + \omega^{2}\boldsymbol{\varphi}_{h}^{\alpha T}\mathbf{m}^{\alpha}\boldsymbol{\varphi}_{co}^{\alpha})\overline{\mathbf{u}}_{c}^{\alpha} + \boldsymbol{\varphi}_{h}^{\alpha T}\overline{\mathbf{f}}^{\alpha}] \tag{45b}$$

$$\overline{\mathbf{u}}_{l}^{\beta} = (\boldsymbol{\Lambda}_{l}^{\beta} + j\omega\boldsymbol{\varphi}_{l}^{\beta T}\mathbf{c}^{\beta}\boldsymbol{\varphi}_{l}^{\beta} - \omega^{2}\mathbf{I}_{l}^{\beta})^{-1}[(-j\omega\boldsymbol{\varphi}_{l}^{\beta T}\mathbf{c}^{\beta}\boldsymbol{\varphi}_{co}^{\beta} + \omega^{2}\boldsymbol{\varphi}_{l}^{\beta T}\mathbf{m}^{\beta}\boldsymbol{\varphi}_{co}^{\beta})\overline{\mathbf{u}}_{c}^{\beta} + \boldsymbol{\varphi}_{l}^{\beta T}\overline{\mathbf{f}}^{\beta}] \tag{46a}$$

$$\overline{\mathbf{u}}_{h}^{\beta} = (\boldsymbol{\Lambda}_{h}^{\beta} + j\omega\boldsymbol{\varphi}_{h}^{\beta T}\mathbf{c}^{\beta}\boldsymbol{\varphi}_{h}^{\beta} - \omega^{2}\mathbf{I}_{h}^{\beta})^{-1}[(-j\omega\boldsymbol{\varphi}_{h}^{\beta T}\mathbf{c}^{\beta}\boldsymbol{\varphi}_{co}^{\beta} + \omega^{2}\boldsymbol{\varphi}_{h}^{\beta T}\mathbf{m}^{\beta}\boldsymbol{\varphi}_{co}^{\beta})\overline{\mathbf{u}}_{c}^{\beta} + \boldsymbol{\varphi}_{h}^{\beta T}\overline{\mathbf{f}}^{\beta}] \tag{46b}$$

It is assumed that the substructural lower-order, mid-order and higher-order normal modes have the orthogonality relations with respect to substructural damping matrix. By substituting expressions (45) and (46) into Eqs. (43a) and (43b), respectively, the transformed substructure displacements are rigorously rewritten in the condensation form

$$\overline{\mathbf{X}}^{\alpha} = \boldsymbol{\varphi}_{cc}^{\alpha}\overline{\mathbf{u}}_{c}^{\alpha} + \boldsymbol{\varphi}_{m}^{\alpha}\overline{\mathbf{u}}_{m}^{\alpha} + \boldsymbol{\varphi}_{f}^{\alpha}\overline{\mathbf{f}}^{\alpha} \tag{47a}$$

$$\overline{\mathbf{X}}^{\beta} = \boldsymbol{\varphi}_{cc}^{\beta}\overline{\mathbf{u}}_{c}^{\beta} + \boldsymbol{\varphi}_{m}^{\beta}\overline{\mathbf{u}}_{m}^{\beta} + \boldsymbol{\varphi}_{f}^{\beta}\overline{\mathbf{f}}^{\beta} \tag{47b}$$

where the coefficient matrices

$$\boldsymbol{\varphi}_{cc}^{\alpha}(\omega) = \boldsymbol{\varphi}_{co}^{\alpha} + \omega^{2}(\boldsymbol{\psi}_{lc}^{\alpha} + \boldsymbol{\psi}_{hc}^{\alpha})\mathbf{m}^{\alpha}\boldsymbol{\varphi}_{co}^{\alpha} - j\omega(\boldsymbol{\psi}_{lc}^{\alpha} + \boldsymbol{\psi}_{hc}^{\alpha})\mathbf{c}^{\alpha}\boldsymbol{\varphi}_{co}^{\alpha} \tag{48a}$$

$$\boldsymbol{\varphi}_{f}^{\alpha}(\omega) = \boldsymbol{\psi}_{lc}^{\alpha} + \boldsymbol{\psi}_{hc}^{\alpha} = \mathbf{G}_{c}^{\alpha}(\omega) - \boldsymbol{\varphi}_{m}^{\alpha}(\boldsymbol{\Lambda}_{m}^{\alpha} + j\omega\boldsymbol{\varphi}_{m}^{\alpha T}\mathbf{c}^{\alpha}\boldsymbol{\varphi}_{m}^{\alpha} - \omega^{2}\mathbf{I}_{m}^{\alpha})^{-1}\boldsymbol{\varphi}_{m}^{\alpha T} \tag{48b}$$

$$\mathbf{G}_{c}^{\alpha}(\omega) = \begin{bmatrix} (\mathbf{k}_{II}^{\alpha} + j\omega\mathbf{c}_{II}^{\alpha} - \omega^{2}\mathbf{m}_{II}^{\alpha})^{-1} & 0 \\ 0 & 0 \end{bmatrix} \tag{48c}$$

$$\boldsymbol{\varphi}_{cc}^{\beta}(\omega) = \boldsymbol{\varphi}_{co}^{\beta} + \omega^2(\boldsymbol{\psi}_{lc}^{\beta} + \boldsymbol{\psi}_{hc}^{\beta})\mathbf{m}^{\beta}\boldsymbol{\varphi}_{co}^{\beta} - j\omega(\boldsymbol{\psi}_{lc}^{\beta} + \boldsymbol{\psi}_{hc}^{\beta})\mathbf{c}^{\beta}\boldsymbol{\varphi}_{co}^{\beta} \tag{49a}$$

$$\boldsymbol{\varphi}_{f}^{\beta}(\omega) = \boldsymbol{\psi}_{lc}^{\beta} + \boldsymbol{\psi}_{hc}^{\beta} = \mathbf{G}_{c}^{\beta}(\omega) - \boldsymbol{\varphi}_{m}^{\beta}(\boldsymbol{\Lambda}_{m}^{\beta} + j\omega\boldsymbol{\varphi}_{m}^{\beta T}\mathbf{c}^{\beta}\boldsymbol{\varphi}_{m}^{\beta} - \omega^2\mathbf{I}_{m}^{\beta})^{-1}\boldsymbol{\varphi}_{m}^{\beta T} \tag{49b}$$

$$\mathbf{G}_{c}^{\beta}(\omega) = \begin{bmatrix} (\mathbf{k}_{II}^{\beta} + j\omega\mathbf{c}_{II}^{\beta} - \omega^2\mathbf{m}_{II}^{\beta})^{-1} & 0 \\ 0 & 0 \end{bmatrix} \tag{49c}$$

The substructural interface displacements corresponding to expressions (47) are

$$\bar{\mathbf{X}}_{J}^{\alpha} = \bar{\mathbf{u}}_{c}^{\alpha}, \quad \bar{\mathbf{X}}_{J}^{\beta} = \bar{\mathbf{u}}_{c}^{\beta} \tag{50a,b}$$

In terms of structural external forces and internal forces, the transformed substructural external forces are partitioned into

$$\bar{\mathbf{f}}^{\alpha} = \bar{\mathbf{f}}_{E}^{\alpha} + \bar{\mathbf{f}}_{sJ}^{\alpha}, \quad \bar{\mathbf{f}}^{\beta} = \bar{\mathbf{f}}_{E}^{\beta} + \bar{\mathbf{f}}_{sJ}^{\beta} \tag{51a,b}$$

where $\bar{\mathbf{f}}_{E}^{\alpha}$ and $\bar{\mathbf{f}}_{E}^{\beta}$ are the sub-vectors of structural external forces acting on substructures α and β, respectively, $\bar{\mathbf{f}}_{sJ}^{\alpha}$ and $\bar{\mathbf{f}}_{sJ}^{\beta}$ are interaction force vectors between adjacent substructures with zero elements for the non-interface DOFs, that is, $\bar{\mathbf{f}}_{sJ}^{r} = [0 \ \ \bar{\mathbf{f}}_{J}^{rT}]^{T}$ ($r = \alpha, \beta$). Substituting expressions (47) and (51) into Eqs. (43a) and (43b), respectively, premultiplying the resultant equations by the transposed mode matrices $\boldsymbol{\varphi}_{cc}^{\alpha T}$ and $\boldsymbol{\varphi}_{cc}^{\beta T}$, and using the orthogonality relations (6) yield

$$\bar{\mathbf{f}}_{J}^{\alpha} = \boldsymbol{\varphi}_{cc}^{\alpha T}\bar{\mathbf{f}}_{sJ}^{\alpha} = \boldsymbol{\varphi}_{cc}^{\alpha T}\mathbf{K}_{c}^{\alpha}(\boldsymbol{\varphi}_{cc}^{\alpha}\bar{\mathbf{u}}_{c}^{\alpha} + \boldsymbol{\varphi}_{m}^{\alpha}\bar{\mathbf{u}}_{m}^{\alpha}) + \boldsymbol{\varphi}_{cc}^{\alpha T}(\mathbf{K}_{c}^{\alpha}\boldsymbol{\varphi}_{f}^{\alpha} - \mathbf{I}^{\alpha})\bar{\mathbf{f}}_{E}^{\alpha} \tag{52a}$$

$$\bar{\mathbf{f}}_{J}^{\beta} = \boldsymbol{\varphi}_{cc}^{\beta T}\bar{\mathbf{f}}_{sJ}^{\beta} = \boldsymbol{\varphi}_{cc}^{\beta T}\mathbf{K}_{c}^{\beta}(\boldsymbol{\varphi}_{cc}^{\beta}\bar{\mathbf{u}}_{c}^{\beta} + \boldsymbol{\varphi}_{m}^{\beta}\bar{\mathbf{u}}_{m}^{\beta}) + \boldsymbol{\varphi}_{cc}^{\beta T}(\mathbf{K}_{c}^{\beta}\boldsymbol{\varphi}_{f}^{\beta} - \mathbf{I}^{\beta})\bar{\mathbf{f}}_{E}^{\beta} \tag{52b}$$

with

$$\mathbf{K}_{c}^{\alpha}(\omega) = \mathbf{k}^{\alpha} + j\omega\mathbf{c}^{\alpha} - \omega^2\mathbf{m}^{\alpha}, \quad \mathbf{K}_{c}^{\beta}(\omega) = \mathbf{k}^{\beta} + j\omega\mathbf{c}^{\beta} - \omega^2\mathbf{m}^{\beta} \tag{53a,b}$$

For the adjacent substructures α and β, the displacements compatibility and forces equilibrium at the interface give

$$\bar{\mathbf{X}}_{J}^{\alpha} = \bar{\mathbf{X}}_{J}^{\beta}, \quad \bar{\mathbf{f}}_{J}^{\alpha} + \bar{\mathbf{f}}_{J}^{\beta} = 0 \tag{54a,b}$$

By substituting the expressions of interface displacements (50) and forces (52) into Eq. (54), the transformed substructural interface displacements are obtained as

$$\bar{\mathbf{u}}_{c}^{\alpha} = \bar{\mathbf{u}}_{c}^{\beta} = -\mathbf{g}_{cc}(\mathbf{K}_{cm}^{\alpha}\bar{\mathbf{u}}_{m}^{\alpha} + \mathbf{K}_{cm}^{\beta}\bar{\mathbf{u}}_{m}^{\beta}) - \mathbf{g}_{cc}(\mathbf{K}_{cf}^{\alpha}\bar{\mathbf{f}}_{E}^{\alpha} + \mathbf{K}_{cf}^{\beta}\bar{\mathbf{f}}_{E}^{\beta}) \tag{55}$$

where

$$\mathbf{g}_{cc}(\omega) = (\boldsymbol{\varphi}_{cc}^{\alpha T}\mathbf{K}_{c}^{\alpha}\boldsymbol{\varphi}_{cc}^{\alpha} + \boldsymbol{\varphi}_{cc}^{\beta T}\mathbf{K}_{c}^{\beta}\boldsymbol{\varphi}_{cc}^{\beta})^{-1} \tag{56}$$

$$\mathbf{K}_{cm}^{\alpha}(\omega) = \boldsymbol{\varphi}_{cc}^{\alpha T}\mathbf{K}_{c}^{\alpha}\boldsymbol{\varphi}_{m}^{\alpha}, \quad \mathbf{K}_{cm}^{\beta}(\omega) = \boldsymbol{\varphi}_{cc}^{\beta T}\mathbf{K}_{c}^{\beta}\boldsymbol{\varphi}_{m}^{\beta} \tag{57a,b}$$

$$\mathbf{K}_{cf}^{\alpha}(\omega) = \boldsymbol{\varphi}_{cc}^{\alpha T}(\mathbf{K}_{c}^{\alpha}\boldsymbol{\varphi}_{f}^{\alpha}-\mathbf{I}^{\alpha}), \quad \mathbf{K}_{cf}^{\beta}(\omega) = \boldsymbol{\varphi}_{cc}^{\beta T}(\mathbf{K}_{c}^{\beta}\boldsymbol{\varphi}_{f}^{\beta}-\mathbf{I}^{\beta}) \tag{58a,b}$$

According to Eq. (55), the exact condensation transformations for substructural mode displacements are given by

$$\bar{\mathbf{u}}^{\alpha} = \mathbf{T}_{X}^{\alpha}\bar{\mathbf{U}}+\mathbf{T}_{f}^{\alpha}\bar{\mathbf{F}}_{E}, \quad \bar{\mathbf{u}}^{\beta} = \mathbf{T}_{X}^{\beta}\bar{\mathbf{U}}+\mathbf{T}_{f}^{\beta}\bar{\mathbf{F}}_{E} \tag{59a,b}$$

where $\bar{\mathbf{u}}^{\alpha}$ and $\bar{\mathbf{u}}^{\beta}$ are the Fourier transformations of substructural mode displacement vectors $\mathbf{u}^{\alpha}$ and $\mathbf{u}^{\beta}$ (19), respectively, $\bar{\mathbf{U}}$ is the Fourier transformation of all-substructural mid-order mode displacement vector $\mathbf{U}$ (29), the substructural displacement condensation transformation matrices and transformed external force vector are

$$\mathbf{T}_{X}^{\alpha}(\omega) = \begin{bmatrix} -\mathbf{g}_{cc}\mathbf{K}_{cm}^{\alpha} & -\mathbf{g}_{cc}\mathbf{K}_{cm}^{\beta} \\ \mathbf{I}_{m}^{\alpha} & 0 \end{bmatrix}, \quad \mathbf{T}_{f}^{\alpha}(\omega) = \begin{bmatrix} -\mathbf{g}_{cc}\mathbf{K}_{cf}^{\alpha} & -\mathbf{g}_{cc}\mathbf{K}_{cf}^{\beta} \\ 0^{\alpha} & 0 \end{bmatrix} \tag{60a,b}$$

$$\mathbf{T}_{X}^{\beta}(\omega) = \begin{bmatrix} -\mathbf{g}_{cc}\mathbf{K}_{cm}^{\alpha} & -\mathbf{g}_{cc}\mathbf{K}_{cm}^{\beta} \\ 0 & \mathbf{I}_{m}^{\beta} \end{bmatrix}, \quad \mathbf{T}_{f}^{\beta}(\omega) = \begin{bmatrix} -\mathbf{g}_{cc}\mathbf{K}_{cf}^{\alpha} & -\mathbf{g}_{cc}\mathbf{K}_{cf}^{\beta} \\ 0 & 0^{\beta} \end{bmatrix} \tag{61a,b}$$

$$\bar{\mathbf{F}}_{E} = [\bar{\mathbf{f}}_{E}^{\alpha T} \quad \bar{\mathbf{f}}_{E}^{\beta T}]^{T} \tag{62}$$

The substructural displacement expressions (47) can be condensed further and the interface DOFs can be eliminated by the transformations (59). Substituting the substructural displacements (47) and transformations (59) into Eqs. (43a) and (43b), and premultiplying the resultant equations by the transposed matrices $(\boldsymbol{\varphi}_{cm}^{\alpha}\mathbf{T}_{X}^{\alpha})^{T}$ and $(\boldsymbol{\varphi}_{cm}^{\beta}\mathbf{T}_{X}^{\beta})^{T}$, respectively, yield

$$\mathbf{T}_{X}^{\alpha T}\boldsymbol{\varphi}_{cm}^{\alpha T}\mathbf{K}_{c}^{\alpha}\boldsymbol{\varphi}_{cm}^{\alpha}\mathbf{T}_{X}^{\alpha}\bar{\mathbf{U}} = \mathbf{T}_{X}^{\alpha T}\boldsymbol{\varphi}_{cm}^{\alpha T}(\mathbf{I}_{E}^{\alpha} - \mathbf{K}_{c}^{\alpha}\boldsymbol{\varphi}_{f}^{\alpha} - \mathbf{K}_{c}^{\alpha}\boldsymbol{\varphi}_{cm}^{\alpha}\mathbf{T}_{f}^{\alpha})\bar{\mathbf{F}}_{E} + \mathbf{T}_{X}^{\alpha T}\boldsymbol{\varphi}_{cm}^{\alpha \mathrm{T}}\bar{\mathbf{f}}_{sJ}^{\alpha} \tag{63a}$$

$$\mathbf{T}_{X}^{\beta T}\boldsymbol{\varphi}_{cm}^{\beta T}\mathbf{K}_{c}^{\beta}\boldsymbol{\varphi}_{cm}^{\beta}\mathbf{T}_{X}^{\beta}\bar{\mathbf{U}} = \mathbf{T}_{X}^{\beta T}\boldsymbol{\varphi}_{cm}^{\beta T}(\mathbf{I}_{E}^{\beta} - \mathbf{K}_{c}^{\beta}\boldsymbol{\varphi}_{f}^{\beta} - \mathbf{K}_{c}^{\beta}\boldsymbol{\varphi}_{cm}^{\beta}\mathbf{T}_{f}^{\beta})\bar{\mathbf{F}}_{E} + \mathbf{T}_{X}^{\beta T}\boldsymbol{\varphi}_{cm}^{\beta T}\bar{\mathbf{f}}_{sJ}^{\beta} \tag{63b}$$

with

$$\boldsymbol{\varphi}_{cm}^{\alpha} = [\boldsymbol{\varphi}_{cc}^{\alpha} \ \ \boldsymbol{\varphi}_{m}^{\alpha}], \quad \boldsymbol{\varphi}_{cm}^{\beta} = [\boldsymbol{\varphi}_{cc}^{\beta} \ \ \boldsymbol{\varphi}_{m}^{\beta}] \tag{64a,b}$$

$$\mathbf{I}_{E}^{\alpha} = \mathrm{diag}[\mathbf{I}^{\alpha}, 0], \quad \mathbf{I}_{E}^{\beta} = \mathrm{diag}[0, \mathbf{I}^{\beta}] \tag{64c,d}$$

Eqs. (63a) and (63b) exactly describe the function relations of frequency-response to external excitation for substructures α and β, respectively, in which only DOFs relative to substructural mid-order modes are retained. Under the forces equilibrium of adjacent substructures (54b), there exists

$$\mathbf{T}_{X}^{\alpha T}\boldsymbol{\varphi}_{cm}^{\alpha T}\bar{\mathbf{f}}_{sJ}^{\alpha}+\mathbf{T}_{X}^{\beta T}\boldsymbol{\varphi}_{cm}^{\beta T}\bar{\mathbf{f}}_{sJ}^{\beta} = 0 \tag{65}$$

Then the entire-structural frequency-response equation is obtained by assembling substructural Eqs. (63a) and (63b) and using Eq. (65) in the exact condensation form

$$\mathbf{K}_u\overline{\mathbf{U}} = \mathbf{K}_f\overline{\mathbf{F}}_E \tag{66}$$

where the synthesized structure coefficient matrices

$$\mathbf{K}_u(\omega) = \mathbf{T}_X^{\alpha T}\boldsymbol{\varphi}_{cm}^{\alpha T}\mathbf{K}_c^{\alpha}\boldsymbol{\varphi}_{cm}^{\alpha}\mathbf{T}_X^{\alpha} + \mathbf{T}_X^{\beta T}\boldsymbol{\varphi}_{cm}^{\beta T}\mathbf{K}_c^{\beta}\boldsymbol{\varphi}_{cm}^{\beta}\mathbf{T}_X^{\beta} \tag{67a}$$

$$\mathbf{K}_f(\omega) = \mathbf{T}_X^{\alpha T}\boldsymbol{\varphi}_{cm}^{\alpha T}(\mathbf{I}_E^{\alpha} - \mathbf{K}_c^{\alpha}\boldsymbol{\varphi}_f^{\alpha} - \mathbf{K}_c^{\alpha}\boldsymbol{\varphi}_{cm}^{\alpha}\mathbf{T}_f^{\alpha}) + \mathbf{T}_X^{\beta T}\boldsymbol{\varphi}_{cm}^{\beta T}(\mathbf{I}_E^{\beta} - \mathbf{K}_c^{\beta}\boldsymbol{\varphi}_f^{\beta} - \mathbf{K}_c^{\beta}\boldsymbol{\varphi}_{cm}^{\beta}\mathbf{T}_f^{\beta}) \tag{67b}$$

The generalized frequency-response function matrix for the synthesized structure is derived from Eq. (66) as

$$\mathbf{H}_g(\omega) = \mathbf{K}_u^{-1}(\omega)\mathbf{K}_f(\omega) \tag{68}$$

which represents the exact substructural mid-order mode displacement responses to external pulse excitations in frequency domain and can be calculated directly. The generalized frequency-response function matrix $\mathbf{H}_g$ has the number of row equal to that of total substructural mid-order modes. The original entire structural frequency-response function matrix $\mathbf{H}$ can be obtained by assembling substructural frequency-response function matrices $\mathbf{H}^{\alpha}$ and $\mathbf{H}^{\beta}$. The substructural frequency-response function matrices or the substructural displacement responses to external pulse excitations in frequency domain are obtained by substituting Eqs. (59) and (66) into expressions (47) and using the generalized frequency-response functions (68) as

$$\mathbf{H}^{\alpha}(\omega) = \boldsymbol{\varphi}_{cm}^{\alpha}(\mathbf{T}_X^{\alpha}\mathbf{H}_g + \mathbf{T}_f^{\alpha}) + \boldsymbol{\varphi}_{fE}^{\alpha} \tag{69a}$$

$$\mathbf{H}^{\beta}(\omega) = \boldsymbol{\varphi}_{cm}^{\beta}(\mathbf{T}_X^{\beta}\mathbf{H}_g + \mathbf{T}_f^{\beta}) + \boldsymbol{\varphi}_{fE}^{\beta} \tag{69b}$$

where the substructural residual flexibility matrices

$$\boldsymbol{\varphi}_{fE}^{\alpha}(\omega) = [\boldsymbol{\varphi}_f^{\alpha}\ \ 0], \quad \boldsymbol{\varphi}_{fE}^{\beta}(\omega) = [0\ \ \boldsymbol{\varphi}_f^{\beta}] \tag{70a,b}$$

Thus the entire-structural frequency-response functions can be determined as follows: (I) calculating the condensed generalized structural frequency-response functions (68); (II) calculating respectively the substructural frequency-response functions (69) to form structural frequency-response function matrix.

5. Substructures coupling for exact response statistics

The structural random response can be obtained by assembling substructural random responses. The substructural random responses can be estimated by using the frequency-response functions and the power spectral density functions. For simplicity, consider two adjacent substructures coupling, in which substructures α and β have a common interface. The coupling procedure can be extended to the case with more than two substructures.

In frequency domain, the substructure displacements can be expressed exactly as Eq. (44). They can be reduced exactly to Eq. (47) by using the substructural dynamic equations, and further reduced exactly by using the transformations (59) derived from the substructural interfacial displacements compatibility and forces equilibrium. The reduced displacement expressions retain only DOFs relative to substructural mid-order modes, and the substructural lower/higher-order normal modes and constraint modes relative to interface DOFs are involved in the relevant coefficients.

The substructural frequency-response function equations can be given in the exact condensation form as Eq. (63) by using the exact reduced displacements and dynamic equations. These equations can be assembled into structural frequency-response function Eq. (66), and then the generalized synthesized structural frequency-response functions are obtained as Eq. (68). The substructural frequency-response functions are further obtained exactly as Eq. (69), which can form entire-structural frequency-response function matrix.

By using the frequency-response functions (69), the power spectral density functions for substructures α and β can be expressed as

$$\mathbf{S}^{\alpha}(\omega) = \mathbf{H}^{\alpha}(\omega)\mathbf{S}_F(\omega)[\mathbf{H}^{\alpha}(\omega)]^{*T} \tag{71a}$$

$$\mathbf{S}^{\beta}(\omega) = \mathbf{H}^{\beta}(\omega)\mathbf{S}_F(\omega)[\mathbf{H}^{\beta}(\omega)]^{*T} \tag{71b}$$

$$\mathbf{S}^{\alpha\beta}(\omega) = \mathbf{H}^{\alpha}(\omega)\mathbf{S}_F(\omega)[\mathbf{H}^{\beta}(\omega)]^{*T} \tag{71c}$$

where superscript * denotes the complex conjugation, $\mathbf{S}_F(\omega)$ is the structural external-excitation spectral-density matrix, $\mathbf{S}^{\alpha}(\omega)$ and $\mathbf{S}^{\beta}(\omega)$ are the auto-power spectral density matrices of substructures α and β, respectively, and $\mathbf{S}^{\alpha\beta}(\omega)$ is the cross-power spectral density matrix of two substructures. Then the displacement correlation functions for substructures α and β are given by

$$\mathbf{R}_X^{\alpha}(0) = E[\mathbf{X}^{\alpha}\mathbf{X}^{\alpha T}] = 2\int_0^{\infty}\mathbf{S}^{\alpha}(\omega)d\omega \tag{72a}$$

$$\mathbf{R}_X^{\beta}(0) = E[\mathbf{X}^{\beta}\mathbf{X}^{\beta T}] = 2\int_0^{\infty}\mathbf{S}^{\beta}(\omega)d\omega \tag{72b}$$

$$\mathbf{R}_X^{\alpha\beta}(0) = E[\mathbf{X}^{\beta}\mathbf{X}^{\beta T}] = 2\int_0^{\infty}\mathbf{S}^{\alpha\beta}(\omega)d\omega \tag{72c}$$

where $E[\cdot]$ denotes the expectation operator, $\mathbf{R}_X^{\alpha}$ and $\mathbf{R}_X^{\beta}$ are the auto-correlation function matrices of substructures α and β, respectively, and $\mathbf{R}_X^{\alpha\beta}$ is the cross-correlation function matrix of two substructures. The integral interval can be determined finitely according to the substructural power spectral density functions or the structural external-excitation spectral-density functions.

The structural mean-square displacements or the substructural mean-square displacements can be obtained from the diagonal elements of the auto-correlation function matrices, that is

$$E[(X_i^{\alpha})^2] = (\mathbf{R}_X^{\alpha})_{ii} = 2\int_0^{\infty}[\mathbf{S}^{\alpha}(\omega)]_{ii}d\omega \tag{73a}$$

$$E[(X_i^{\beta})^2] = (\mathbf{R}_X^{\beta})_{ii} = 2\int_0^{\infty}[\mathbf{S}^{\beta}(\omega)]_{ii}d\omega \tag{73b}$$

$$i = 1, 2, \ldots$$

where X_i^{α} and X_i^{β} are the i-th elements of substructural displacement vectors $\mathbf{X}^{\alpha}$ and $\mathbf{X}^{\beta}$, respectively. Similarly, the substructural mean-square accelerations can be obtained as

$$E[(\ddot{X}_i^{\alpha})^2] = 2\int_0^{\infty}\omega^4[\mathbf{S}^{\alpha}(\omega)]_{ii}d\omega \tag{74a}$$

$$E[(\ddot{X}_i^{\beta})^2] = 2\int_0^{\infty}\omega^4[\mathbf{S}^{\beta}(\omega)]_{ii}d\omega \tag{74b}$$

$$i = 1, 2, \ldots$$

The substructural frequency-response functions corresponding to interface DOFs are elements of the frequency-response matrix (69) and can be given by

$$\mathbf{H}_J^{\alpha}(\omega) = [\mathbf{I}_J^{\alpha}\ \ 0](\mathbf{T}_X^{\alpha}\mathbf{H}_g + \mathbf{T}_f^{\alpha}) \tag{75a}$$

$$\mathbf{H}_J^{\beta}(\omega) = [\mathbf{I}_J^{\beta}\ \ 0](\mathbf{T}_X^{\beta}\mathbf{H}_g + \mathbf{T}_f^{\beta}) \tag{75b}$$

Substituting Eqs. (60) and (61) into Eqs. (75a) and (75b), respectively, yields

$$\mathbf{H}_J^{\alpha}(\omega) = \mathbf{H}_J^{\beta}(\omega) \tag{76}$$

Thus the frequency-response functions for interface DOFs of substructure α are equal to those for corresponding interface DOFs of substructure β. Then the power spectral density functions for interface DOFs of substructure α are equal to those for corresponding interface DOFs of substructure β according to Eqs. (71a) and (71b), that is

$$\mathbf{S}_J^{\alpha}(\omega) = \mathbf{H}_J^{\alpha}\mathbf{S}_F(\mathbf{H}_J^{\alpha})^{*T} = \mathbf{H}_J^{\beta}\mathbf{S}_F(\mathbf{H}_J^{\beta})^{*T} = \mathbf{S}_J^{\beta}(\omega) \tag{77}$$

The response statistics such as mean-square displacements (73a) and mean-square accelerations (74a) for interface DOFs of substructure α are equal to those in Eqs. (73b) and (74b) for corresponding interface DOFs of substructure β, respectively.

6. Numerical examples and results

The above developed accurate substructural synthesis method for structural mid-order modes, frequency-response functions and random responses is applied to a beam and a plate, respectively. Numerical results are obtained to illustrate the synthesis accuracy and capacity, which are given as follows: mid-order mode synthesis, frequency-response function synthesis and random response synthesis.

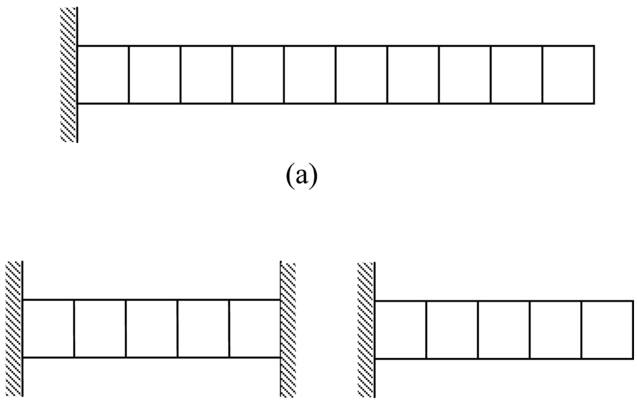

(a)

(b) (c)

Fig. 1 Cantilever beam with two substructures (a) beam, (b) substructure 1, (c) substructure 2

Table 1 Substructural natural frequencies of the beam (Hz)

Order	Substructure 1	Substructure 2	Order	Substructure 1	Substructure 2
1	58.1	9.1	6	1291.2	856.7
2	160.4	57.2	7	1883.4	1241.0
3	316.5	160.1	8	2621.9	1778.4
4	524.6	314.9	9	\	2488.8
5	874.8	519.7	10	\	3453.0

Table 2 Synthesized natural frequencies of the beam (Hz)

Retained 6-7th frequencies of substructure 1	Retained 8-9th frequencies of substructure 2	Synthesized frequencies	Original frequencies
		362.9	362.9
		468.0	468.0
		580.2	580.2
		769.3	769.3
		925.6	925.6
		1117.2	1117.2
1291.2		1341.9	1341.9
		1603.7	1603.7
1883.4	1778.4	1906.3	1906.3
		2246.9	2246.9
	2488.8	2604.3	2604.3
		2916.2	2916.2
		3459.7	3459.7

6.1 Mid-order mode synthesis

Consider a cantilever beam with the Young's modulus $E = 2$ GPa, mass density $\rho = 4000$ kg/m^3, length $L = 1$ m, cross-sectional height $h = 2$ cm and width $b = 1.5$ cm, as shown in Fig. 1(a). The beam is divided equally into 10 elements and its natural modes in flexural vibration as original results are firstly obtained by using the finite element method. Then the beam is divided into substructure 1 with 5 elements and substructure 2 with 5 elements as shown in Figs. 1(b) and 1(c), respectively. Fixed-interfacial substructure modes are obtained also by the finite element method, as listed in Table 1. By using the developed mode synthesis method, the synthesized natural frequencies of the beam are obtained and compared with the original results as given in Tables 2 and 3 for various substructure modes retained. It is seen from these tables that the synthesized structural natural frequencies are quite equal to the original ones in the sense of assigned accuracy.

Furthermore, consider a plate with the Young's modulus $E = 200$ GPa, Poisson's ratio $\nu = 0.3$, mass density $\rho = 7800$ kg/m^3, length $a = 4$ m, width $b = 1$ m and thickness $h = 4$ cm, as shown in Fig. 2(a). The plate is divided equally into 16 elements and its natural modes in flexural vibration are firstly obtained by using the finite element method. Then the plate is divided into substructures 1 and 2 with 6 elements and substructure 3 with 4 elements as shown in Figs. 2(b), 2(c) and 2(d), respectively. Fixed-interfacial substructure modes are obtained by the finite element method, as listed in Table 4. The synthesized natural frequencies of the plate with the original results are given in Table 5, by which the accuracy of the developed substructural mode synthesis method is verified again.

However, it is important to retain suitable substructural modes used for synthesis. The substructural mode synthesis results including calculating accuracy, efficiency and stability are affected by the retained substructural modes and determined characteristics of the synthesis problem. For example, in Tables 2, 3 and 5, the synthesized lower-order natural frequencies of the beam and plat are unstable in calculation and cannot be obtained under the mode choice above.

Table 3 Synthesized natural frequencies of the beam by retaining substructural discrete-order modes (Hz)

Retained 6th, 8th frequencies of substructure 1	Retained 8th, 10th frequencies of substructure 2	Synthesized frequencies	Original frequencies
		362.9	362.9
		468.0	468.0
		580.2	580.2
		769.3	769.3
		925.6	925.6
		1117.2	1117.2
1291.2		1341.9	1341.9
		1603.7	1603.7
	1778.4	1906.3	1906.3
		2246.9	2246.9
2621.9		2604.3	2604.3
		2916.2	2916.2
	3453.0	3459.7	3459.7

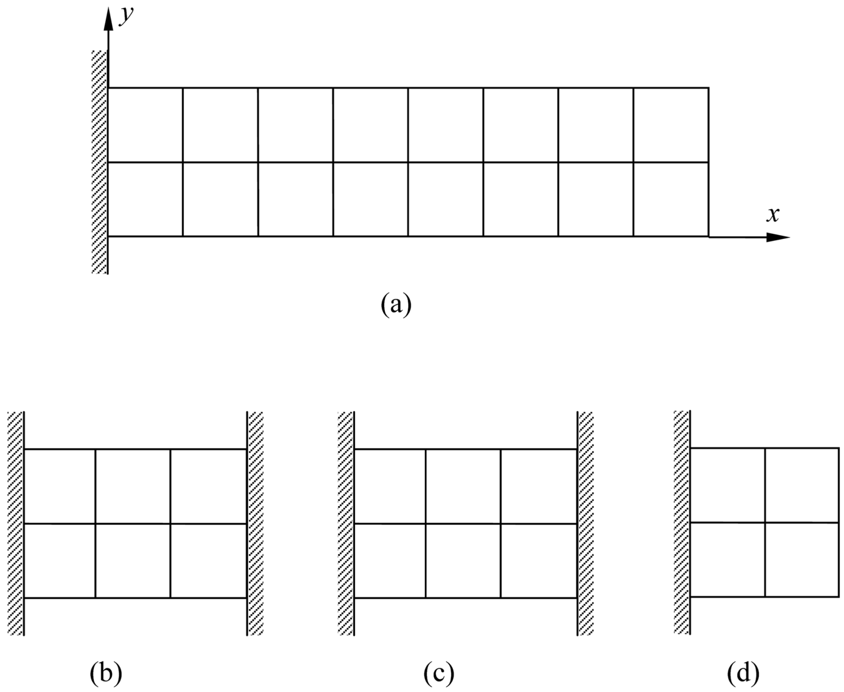

Fig. 2 Plate with three substructures (a) plate, (b) substructure 1, (c) substructure 2, (d) substructure 3

Table 4 Substructural natural frequencies of the plate (Hz)

Order	Substructure 1	Substructure 2	Substructure 3
1	95.2066	95.2066	33.5832
2	138.7720	138.7720	86.0325
3	251.3261	251.3261	205.2708
4	300.8461	300.8461	260.6659
5	301.4684	301.4684	294.5259
6	438.5340	438.5340	454.8520
7	645.9053	645.9053	787.8704
8	706.8991	706.8991	796.4613
9	815.8351	815.8351	825.2874
10	845.5689	845.5689	830.0702
11	863.1778	863.1778	897.3308
12	869.4954	869.4954	1794.2806
13	1023.3880	1023.3880	1932.5770
14	1189.4015	1189.4015	2119.0721
15	2065.9392	2065.9392	2327.0792
16	2127.0904	2127.0904	2513.0088
17	2287.8238	2287.8238	2694.8639
18	2300.8877	2300.8877	3296.1209

Table 5 Synthesized natural frequencies of the plate (Hz)

Synthesized frequencies for retained 11-12th frequencies of three substructures	Synthesized frequencies for retained 11-12th frequencies of substructure 1, 13-14th frequencies of substructures 2 and 3	Synthesized frequencies for retained 11-12th frequencies of substructure 1, 13-14th frequencies of substructure 2 and 15-16th frequencies of substructure 3	Original frequencies
325.0129	325.0129	325.0129	325.0129
371.6492	371.6492	371.6492	371.6492
376.6264	376.6264	376.6264	376.6264
423.8341	423.8341	423.8341	423.8341
464.4841	464.4841	464.4841	464.4841
486.9318	486.9318	486.9318	486.9318
505.7443	505.7443	505.7443	505.7443
618.2218	618.2218	618.2218	618.2218
622.4105	622.4105	622.4105	622.4105
692.2744	692.2744	692.2744	692.2744
772.8413	772.8413	772.8413	772.8413
776.5742	776.5742	776.5742	776.5742
794.1230	794.1230	794.1230	794.1230
797.9250	797.9250	797.9250	797.9250
804.7745	804.7745	804.7745	804.7745
815.0901	815.0901	815.0901	815.0901
821.9671	821.9671	821.9671	821.9671
826.1321	826.1321	826.1321	826.1321
837.4423	837.4423	837.4423	837.4423
842.1329	842.1329	842.1329	842.1329
850.8743	850.8743	850.8743	850.8743
854.7229	854.7229	854.7229	854.7229
861.3470	861.3470	861.3470	861.3470
862.4853	862.4853	862.4853	862.4853
872.1491	872.1491	872.1491	872.1491
883.3355	883.3355	883.3355	883.3355
907.9827	907.9827	907.9827	907.9827
929.3042	929.3042	929.3042	929.3042
976.4722	976.4722	976.4722	976.4722
992.1059	992.1059	992.1059	992.1059
1075.4194	1075.4194	1075.4194	1075.4194
1141.6547	1141.6547	1141.6547	1141.6547
1193.1661	1193.1661	1193.1661	1193.1661
1411.3277	1411.3277	1411.3277	1411.3277
1582.4436	1582.4436	1582.4436	1582.4436
1805.7654	1805.7654	1805.7654	1805.7654
1964.2771	1964.2771	1964.2771	1964.2771
2076.1147	2076.1147	2076.1147	2076.1147

Table 5 Continued

Synthesized frequencies for retained 11-12th frequencies of three substructures	Synthesized frequencies for retained 11-12th frequencies of substructure 1, 13-14th frequencies of substructures 2 and 3	Synthesized frequencies for retained 11-12th frequencies of substructure 1, 13-14th frequencies of substructure 2 and 15-16th frequencies of substructure 3	Original frequencies
2090.9823	2090.9823	2090.9823	2090.9823
2112.5638	2112.5638	2112.5638	2112.5638
2149.0424	2149.0424	2149.0424	2149.0424
2151.3332	2151.3332	2151.3332	2151.3332
2187.0767	2187.0767	2187.0767	2187.0767
2293.3059	2293.3059	2293.3059	2293.3059
2298.3588	2298.3588	2298.3588	2298.3588
2349.5920	2349.5920	2349.5920	2349.5920
2401.3407	2401.3407	2401.3407	2401.3407
2451.4981	2451.4981	2451.4981	2451.4981
2456.2153	2456.2153	2456.2153	2456.2153
2504.5187	2504.5187	2504.5187	2504.5187
2638.7441	2638.7441	2638.7441	2638.7441
2645.7629	2645.7629	2645.7629	2645.7629
2959.7566	2959.7566	2959.7566	2959.7566
3341.6360	3341.6360	3341.6360	3341.6360

6.2 Frequency-response function synthesis

Consider a cantilever beam as described in section 6.1, in which the cross-sectional area $A = 2 \times 10^{-4}\,\text{m}^2$, second area moment $I = 6.67 \times 10^{-9}\,\text{m}^4$, Rayleigh damping coefficients $a = 0.4951$ and $b = 3.8365 \times 10^{-4}$. The beam is divided equally into 10 elements and its frequency-response functions in flexural vibration as original results are firstly obtained by using the finite element method. Then the beam is divided into substructure 1 and substructure 2, as described in section 6.1. Fixed-interfacial undamped substructure modes are obtained as listed in Table 6. By using the developed frequency-response function synthesis method, the synthesized frequency-response functions of the undamped beam are calculated and the natural frequencies are obtained by their peak-value characteristics as given in Table 7, from which the synthesized results are observed in good agreement with the original results. Figs. 3-9 show the synthesized frequency-response functions in matrix $\mathbf{H}$ of the damped beam for various substructure modes retained, which are the same as the original ones. Figs. 10-13 illustrate the synthesized generalized frequency-response functions in matrix $\mathbf{H}_g$ for the 4th and 5th order substructure-1 modes and the 5th and 6th order substructure-2 modes retained, while Figs. 14-16 for the 7th and 8th order substructure-1 modes and the 9th and 10th order substructure-2 modes retained. Obviously, the generalized frequency-response functions are very different in two cases.

Consider a plate as described in section 6.1, in which Rayleigh damping coefficients $a = 0.4511$ and $b = 4.2017 \times 10^{-4}$. The plate is divided equally into 16 elements and its frequency-response

Table 6 Substructural natural frequencies of the undamped beam (Hz)

Order	Substructure 1	Substructure 2	Order	Substructure 1	Substructure 2
1	58.1322	9.1354	6	1291.2287	856.7268
2	160.4341	57.1724	7	1883.3787	1241.0062
3	316.4764	160.0987	8	2621.9128	1778.4312
4	524.5670	314.8786	9	\	2488.8006
5	874.8265	519.7298	10	\	3452.9931

Table 7 Synthesized natural frequencies of the undamped beam from frequency- response functions (Hz)

Order	Synthesized frequencies	Original frequencies	Order	Synthesized frequencies	Original frequencies
1	2.2844	2.2843	11	769.3136	769.3136
2	14.3096	14.3096	12	925.6392	925.6392
3	40.0462	40.0462	13	1117.1934	1117.1934
4	78.4437	78.4437	14	1341.8622	1341.8622
5	129.6921	129.6921	15	1603.7076	1603.7076
6	193.9539	193.9539	16	1906.2780	1906.2780
7	271.5605	271.5605	17	2246.8658	2246.8658
8	362.9371	362.9371	18	2604.2627	2604.2627
9	467.9889	467.9889	19	2916.2322	2916.2322
10	580.1530	580.1530	20	3459.7496	3459.7496

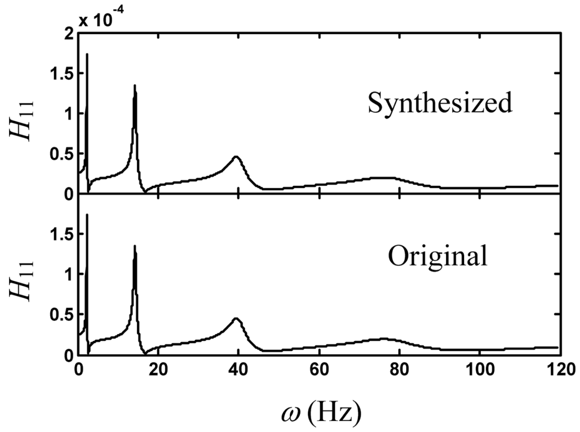

Fig. 3 Synthesized frequency-response function H_{11} of the damped beam

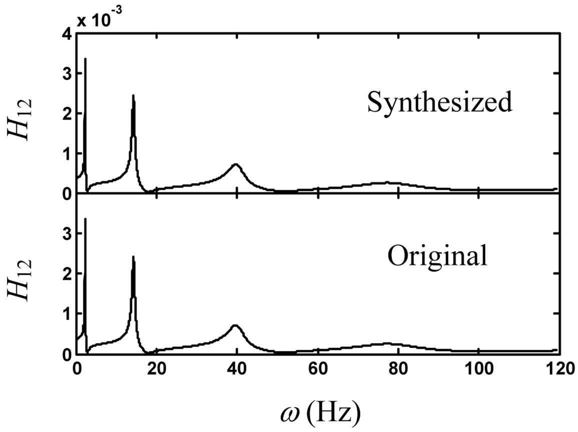

Fig. 4 Synthesized frequency-response function H_{12} of the damped beam

functions in flexural vibration are firstly obtained by the finite element method. Then the plate is divided into substructures 1, 2 and 3 as described in section 6.1. Fixed-interfacial undamped substructure modes are obtained as listed in Table 4. The synthesized frequency-response functions of the damped plate are obtained as shown in Figs. 17-22, by which the accuracy and capacity of the developed substructural frequency-response function synthesis method is verified again.

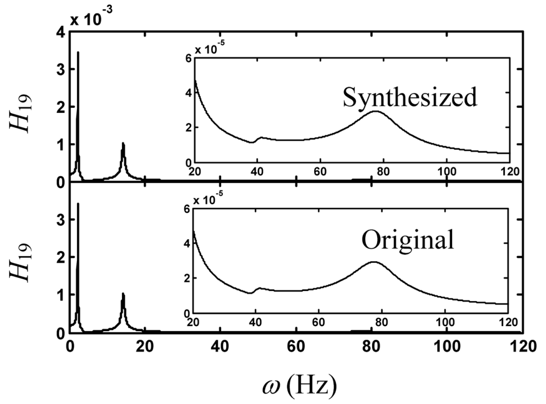

Fig. 5 Synthesized frequency-response function H_{19} of the damped beam

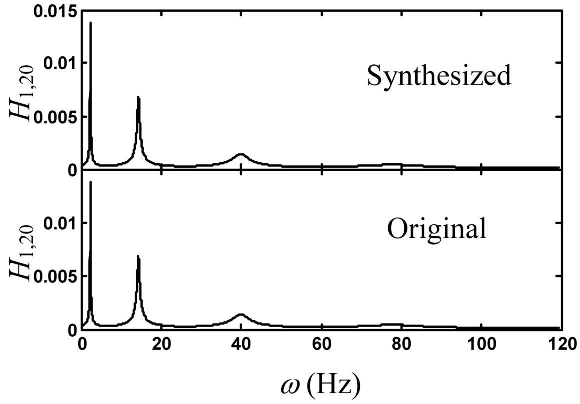

Fig. 6 Synthesized frequency-response function $H_{1,20}$ of the damped beam

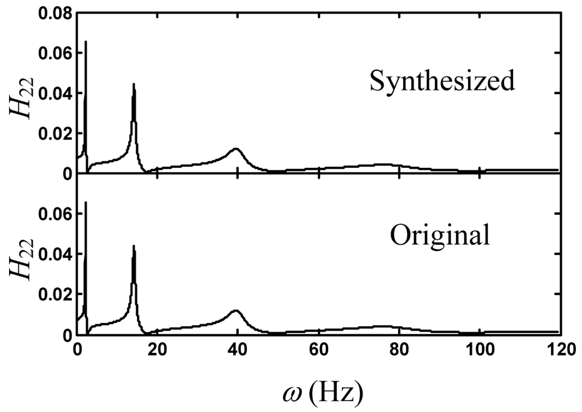

Fig. 7 Synthesized frequency-response function H_{22} of the damped beam

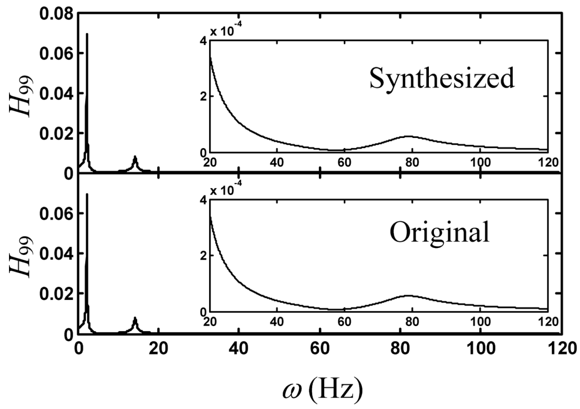

Fig. 8 Synthesized frequency-response function H_{99} of the damped beam

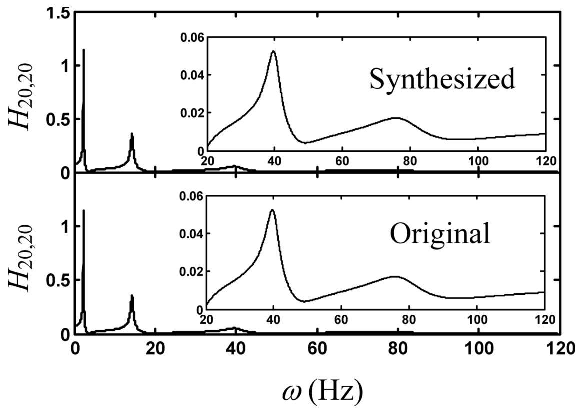

Fig. 9 Synthesized frequency-response function $H_{20,20}$ of the damped beam

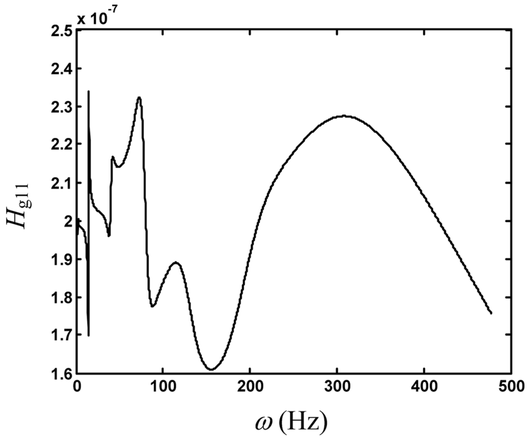

Fig. 10 Synthesized generalized frequency-response function H_{g11} of the beam

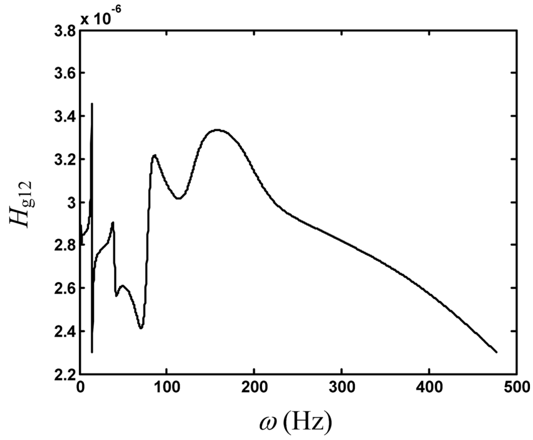

Fig. 11 Synthesized generalized frequency-response function H_{g12} of the beam

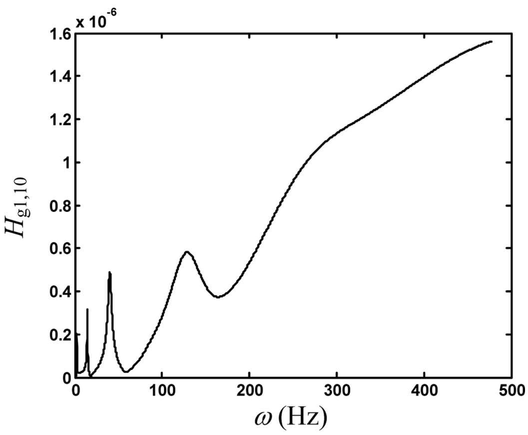

Fig. 12 Synthesized generalized frequency-response function $H_{g1,10}$ of the beam

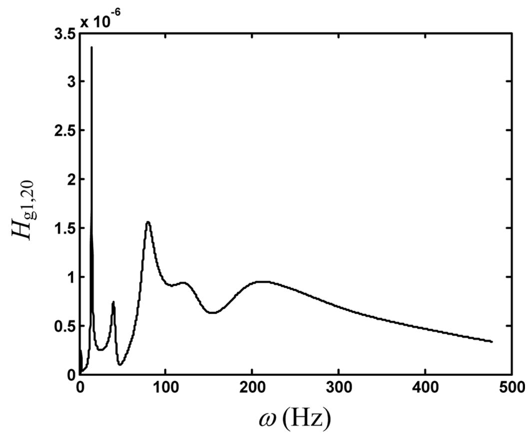

Fig. 13 Synthesized generalized frequency-response function $H_{g1,20}$ of the beam

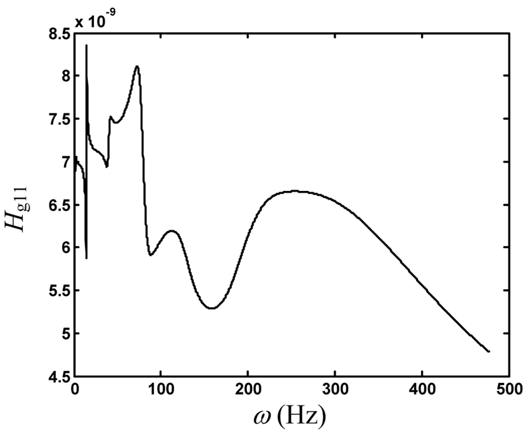

Fig. 14 Synthesized generalized frequency-response function H_{g11} of the beam

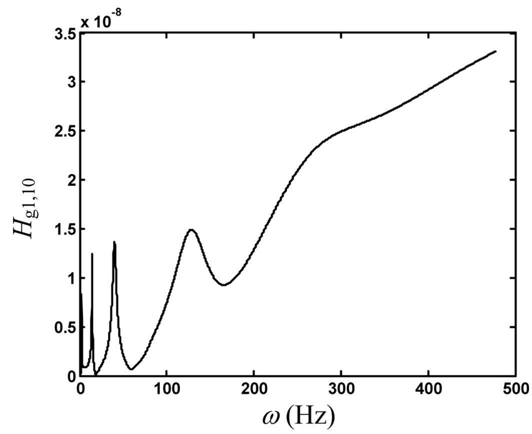

Fig. 15 Synthesized generalized frequency-response function $H_{g1,10}$ of the beam

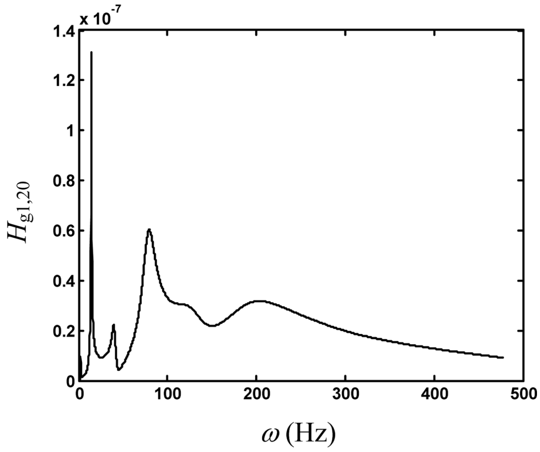

Fig. 16 Synthesized generalized frequency-response function $H_{g1,20}$ of the beam

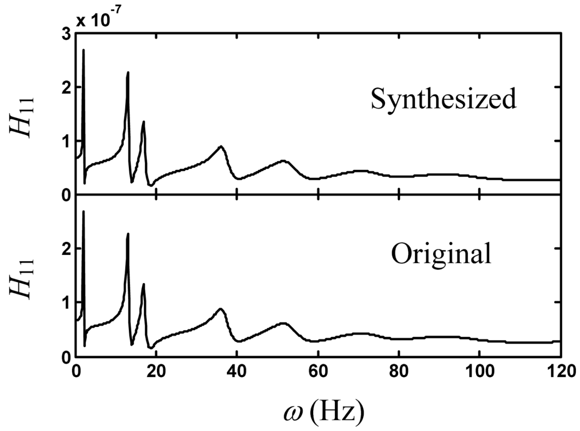

Fig. 17 Synthesized frequency-response function H_{11} of the damped plate

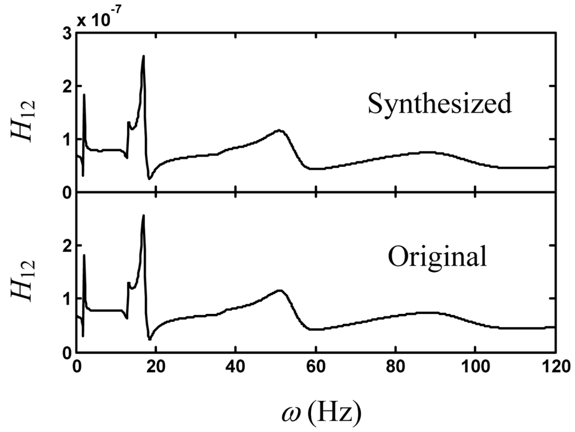

Fig. 18 Synthesized frequency-response function H_{12} of the damped plate

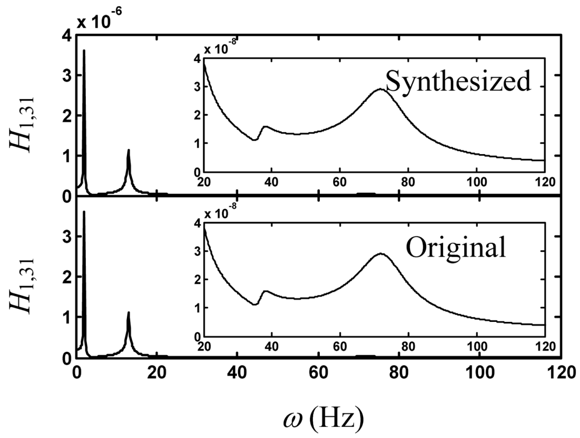

Fig. 19 Synthesized frequency-response function $H_{1,31}$ of the damped plate

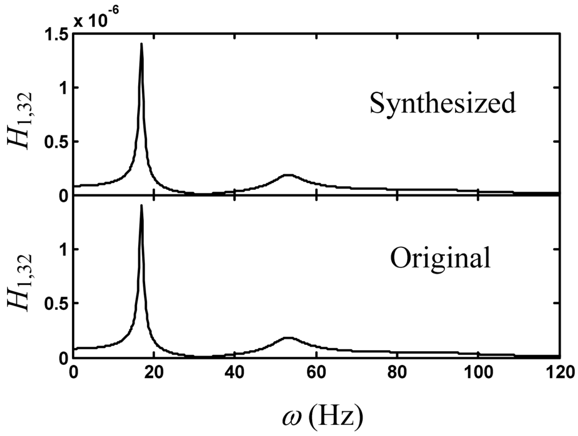

Fig. 20 Synthesized frequency-response function $H_{1,32}$ of the damped plate

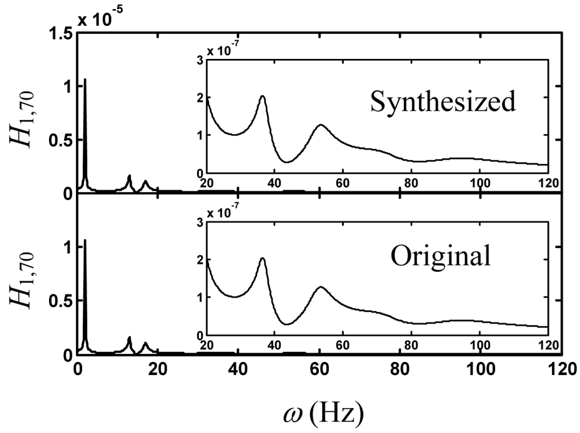

Fig. 21 Synthesized frequency-response function $H_{1,70}$ of the damped plate

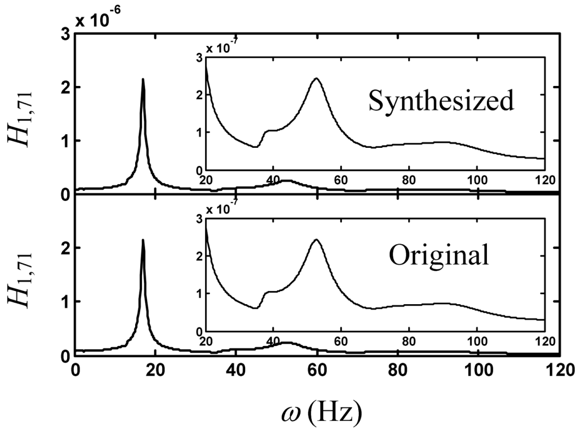

Fig. 22 Synthesized frequency-response function $H_{1,71}$ of the damped plate

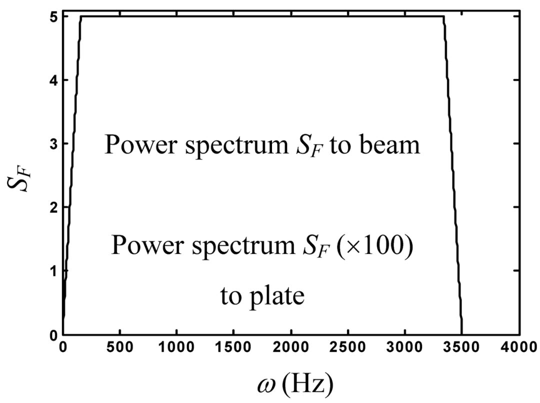

Fig. 23 Power spectral density S_F of random excitations to beam and plate

Table 8 Synthesized mean-square deflections and rotation angles of the beam subjected to a random excitation ($\times 10^{-4}$)

Node	Synthesized		Original	
	Deflection	Rotation angle	Deflection	Rotation angle
1	0.2885	98.3809	0.2885	98.3809
2	3.3828	253.5509	3.3828	253.5509
3	12.9208	400.8449	12.9208	400.8449
4	31.9326	541.9725	31.9326	541.9725
5	63.0772	688.3925	63.0772	688.3925
6	109.1614	844.6930	109.1614	844.6930
7	173.3500	1002.0823	173.3500	1002.0823
8	258.8605	1137.3545	258.8605	1137.3545
9	368.1782	1219.4949	368.1782	1219.4949
10	502.2763	1241.2521	502.2763	1241.2521

Table 9 Synthesized mean-square flexural accelerations ($\times 10^5$) and angular accelerations ($\times 10^7$) of the beam subjected to a random excitation

Node	Synthesized		Original	
	Flexural acceleration	Angular acceleration	Flexural acceleration	Angular acceleration
1	3.2111	4.5132	3.2111	4.5132
2	6.1398	5.6312	6.1398	5.6312
3	4.5983	9.7505	4.5983	9.7505
4	5.8354	12.0388	5.8354	12.0388
5	7.3132	19.3800	7.3132	19.3800
6	10.7690	37.0620	10.7690	37.0620
7	19.3991	102.6249	19.3991	102.6249
8	50.8368	469.7463	50.8368	469.7463
9	200.0488	2939.5724	200.0488	2939.5724
10	6953.0027	52409.2583	6953.0027	52409.2583

Table 10 Synthesized mean-square deflections and rotation angles of the plate subjected to a random excitation ($\times 10^{-9}$)

Node	Synthesized			Original		
	Deflection	Rotation angle (axis x)	Rotation angle (axis y)	Deflection	Rotation angle (axis x)	Rotation angle (axis y)
1	4.3286	6.2310	49.4765	4.3286	6.2310	49.4765
2	3.1319	7.0719	38.2518	3.1319	7.0719	38.2518
3	4.0938	6.2893	47.5004	4.0938	6.2893	47.5004
4	40.8836	37.3091	106.2519	40.8836	37.3091	106.2519
5	32.4790	37.9952	90.3029	32.4790	37.9952	90.3029
6	39.4471	37.1328	103.1214	39.4471	37.1328	103.1214
7	137.9280	86.4557	155.3975	137.9280	86.4557	155.3975
8	116.8456	86.3166	138.9270	116.8456	86.3166	138.9270
9	134.5285	85.9377	151.7445	134.5285	85.9377	151.7445
10	315.7218	143.0220	206.0536	315.7218	143.0220	206.0536
11	279.7090	142.6462	190.3024	279.7090	142.6462	190.3024
12	310.5184	142.3880	202.4231	310.5184	142.3880	202.4231
13	596.4616	200.5590	263.2041	596.4616	200.5590	263.2041
14	545.6889	200.5975	248.0355	545.6889	200.5975	248.0355
15	590.2821	200.2893	259.6170	590.2821	200.2893	259.6170
16	1008.8994	254.3003	320.2270	1008.8994	254.3003	320.2270
17	944.5613	254.3456	306.2594	944.5613	254.3456	306.2594
18	1001.7558	253.0184	315.9473	1001.7558	253.0184	315.9473
19	1582.2227	299.6091	356.6046	1582.2227	299.6091	356.6046
20	1506.0903	297.8722	348.4681	1506.0903	297.8722	348.4681
21	1571.8366	294.2888	360.5593	1571.8366	294.2888	360.5593
22	2331.6199	327.3942	365.9980	2331.6199	327.3942	365.9980
23	2247.5323	330.1829	361.3273	2247.5323	330.1829	361.3273
24	2319.2983	343.3295	388.8424	2319.2983	343.3295	388.8424

Table 11 Synthesized mean-square flexural accelerations and angular accelerations of the plate subjected to a random excitation

Node	Synthesized			Original		
	Flexural acceleration	Angular acceleration (axis x)	Angular acceleration (axis y)	Flexural acceleration	Angular acceleration (axis x)	Angular acceleration (axis y)
1	93.9663	181.5667	332.6055	93.9663	181.5667	332.6055
2	13.8979	335.0376	48.7633	13.8979	335.0376	48.7633
3	55.1192	173.6133	211.8087	55.1192	173.6133	211.8087
4	14.88165	388.5098	750.8104	148.8165	388.5098	750.8104
5	14.7561	513.6165	142.3451	14.7561	513.6165	142.3451
6	104.3533	396.5813	178.0221	104.3533	396.5813	178.0221
7	157.2750	328.2024	1159.9658	157.2750	328.2024	1159.9658
8	16.6687	503.3494	181.5041	16.6687	503.3494	181.5041
9	81.7000	443.6959	480.1265	81.7000	443.6959	480.1265
10	210.8180	454.4697	2061.5957	210.8180	454.4697	2061.5957
11	19.4923	803.5186	280.1805	19.4923	803.5186	280.1805
12	140.2859	714.6186	1065.5075	140.2859	714.6186	1065.5075
13	376.1115	1437.5731	5882.0924	376.1115	1437.5731	5882.0924
14	34.0183	1681.7151	1339.7060	34.0183	1681.7151	1339.7060
15	251.9636	2119.1636	2880.7602	251.9636	2119.1636	2880.7602
16	1006.0817	18646.4068	24139.8964	1006.0817	18646.4068	24139.8964
17	270.9677	11191.6857	15706.8524	270.9677	11191.6857	15706.8524
18	469.4675	11730.2801	26100.0083	469.4675	11730.2801	26100.0083
19	2311.6976	67434.0916	39377.0936	2311.6976	67434.0916	39377.0936
20	2292.6968	282868.6483	273519.8855	2292.6968	282868.6483	273519.8855
21	4151.5343	580677.0481	273006.2982	4151.5343	580677.0481	273006.2982
22	1634.1757	100080.0336	33939.7428	1634.1757	100080.0336	33939.7428
23	4163.6654	276295.4480	524950.0530	4163.6654	276295.4480	524950.0530
24	1990582.7788	71904721.4569	71955880.0654	1990582.7788	71904721.4569	71955880.0654

6.3 Random response synthesis

Consider the same damped cantilever beam and divided substructures in flexural vibration as described in section 6.2. The free end of the beam is subjected to a transverse random excitation with the power spectral density S_F as shown in Fig. 23. The mean-square displacements and accelerations of the beam are firstly obtained by using the finite element method. Then by using the developed random response synthesis method, the synthesized random responses of the beam are obtained for various substructure modes retained. Tables 8 and 9 give the synthesized mean-square displacements and accelerations, respectively, which are quite equal to the original results in the sense of assigned accuracy.

Consider the same damped plate and divided substructures in flexural vibration as described in section 6.2. Nodes are numbered along axes y and x. The 24th node of the plate is subjected to a transverse random excitation with the power spectral density as shown in Fig. 23. The mean-square responses of the plate are firstly obtained by the finite element method. Then the synthesized random responses of the plate are obtained for various substructure modes retained, as given in Tables 10 and 11. The agreement between the synthesized results and original results is observed again, which confirms the accuracy and capacity of the developed substructural random response synthesis method.

7. Conclusions

An accurate substructural synthesis method including random responses synthesis, frequency-response functions synthesis and mid-order modes synthesis has been developed based on rigorous substructural description, dynamic condensation and coupling. The developed synthesis method has main advantages as follows: (I) it is an accurate substructural synthesis method with rigorous substructural description and coupling; (II) substructural interface DOFs are eliminated by interfacial displacements compatibility and forces equilibrium; (III) retained fixed-interfacial mid-order substructure modes and exact residual constraint modes are used for substructural description; (IV) substructural frequency-response functions as well as power spectral density functions and random responses can be calculated separately by the generalized frequency-response functions. Numerical results confirm the good accuracy and capacity of the developed substructural synthesis method.

Acknowledgements

The authors are grateful for the supports from the Zhejiang Provincial Natural Science Foundation of China under Grant No. Y607087, the Scientific Research Fund of Zhejiang Provincial Education Department under Grant No. Y200907048 and the National Natural Science Foundation of China under Grant Nos. 11072215 and 10932009.

References

Barauskas, R. and Barauskiene, R. (2004), "Highly convergent dynamic models obtained by modal synthesis with application to short wave pulse propagation", *Int. J. Numer. Meth. Eng.,* **61**, 2536-2554.

Chen, H.M. and Iranata, D. (2008), "Realistic simulation of reinforced concrete structural systems with combine of simplified and rigorous component model", *Struct. Eng. Mech.,* **30**(5), 619-645.

Craig, Jr., R.R. (1995), "Substructure methods in vibration", *ASME J. Vib. Acoust.*, **117**, 207-213.

Craig, Jr., R.R. and Bampton, M.C.C. (1968), "Coupling of substructures for dynamic analysis", *AIAA J.,* **6**, 1313-1319.

Greif, R. (1986), "Substructuring and component mode synthesis", *Shock Vib. Dig.,* **18**, 3-8.

Hou, S.N. (1969), "Review of modal synthesis techniques and a new approach", *Shock Vib. Bull.,* **40**(Part 4), 25-39.

Hurty, W.C. (1965), "Dynamic analysis of structural systems using component modes", *AIAA J.,* **3**, 678-685.

Ji, L., Mace, B.R. and Pinnington, R.J. (2006), "A mode-based approach for the mid-frequency vibration analysis of coupled long- and short-wavelength structures", *J. Sound Vib.,* **289**, 148-170.

Ko, J.H. and Bai, Z. (2008), "High-frequency response analysis via algebraic substructuring", *Int. J. Numer. Meth. Eng.,* **76**, 295-313.

Liu, Y.X. (2010), "Semi-rigid connection modeling for steel frameworks", *Struct. Eng. Mech.,* **35**(4), 431-457.

Meirovitch, L. and Hale, A.L. (1981), "On the substructure synthesis method", *AIAA J.,* **19**, 940-947.
Petrini, F., Li, H. and Bontempi, F. (2010), "Basis of design and numerical modeling of offshore wind turbines", *Struct. Eng. Mech.,* **36**(5), 599-624.
Qian, D. and Hansen, J.S. (1995), "Substructure synthesis method for frequency response of viscoelastic structures", *AIAA J.,* **33**, 520-527.
Qiu, J.B., Ying, Z.G. and Williams, F.W. (1997), "Exact modal synthesis techniques using residual constraint modes", *Int. J. Numer. Meth. Eng.,* **40**, 2475-2492.
Qiu, J.B., Ying, Z.G. and Yam, L.H. (1997), "New modal synthesis technique using mixed modes", *AIAA J.,* **35**, 1869-1875.
Sarkar, A. and Ghanem, R. (2003), "A substructure approach for the midfrequency vibration of stochastic systems", *J. Acoust. Soc. Am.,* **113**, 1922-1934.
Soize, C. and Mziou, S. (2003), "Dynamic substructuring in the medium-frequency range", *AIAA J.,* **41**, 1113-1118.
Tsuei, Y.G. and Yee, E.K.L. (1990), "Component synthesis method for system transient response", *AIAA J.,* **28**, 1794-1799.